JOURNAL OF THE AERONAUTICAL SCIENCES

VOLUME 10 JULY, 1943 NUMBER 7

Aerodynamic Considerations of Rotors in Hovering and Vertical Climb Conditions

CHARLES H. KAMAN*

United Aircraft Corporation

SUMMARY

This article deals with the application of the results of S. Goldstein to analyses of direct lift rotors in the particular conditions of "hovering flight" and "vertical climb." It is felt that Goldstein's vortex theory will offer definite improvements in particular types of rotor calculations and will, as a part thereof, show more clearly the relative effects of a different number of blades and point the way to optimum aerodynamic design criteria. The theory has been discussed briefly and the principal equations applied.

A working system based on the theory has been set up enabling rapid elemental analyses of rotors in the named conditions. As a practical illustration a study has been prepared showing the optimum distribution of the parameter $(b/D)C_L$ for 2-, 3-, 4-, and 6-bladed rotors operating at or near hovering flight. The results show that a tapered and twisted blade is desirable and that the load distribution shifts slightly toward the tip with an increasing number of blades.

A simplified system in the form of a representative station method has been included for those types of analyses where comparative performance of the principal variables is to be studied. The method is flexible and easily adaptable to a solution of any of the major variables such as diameter, hp., r.p.m., blade characteristics, etc.

It is urged that research programs be initiated for the purposes of verifying the theory and permitting empirical extensions into those analyses that at present involve prohibitive computations.

SYMBOLS

r, R	=	elemental radius and tip radius, respectively
D	=	rotor diameter
b	=	elemental blade width
h	=	elemental blade thickness
B	=	number of blades
w	=	axial velocity component of helicoid
w_i	=	inflow velocity
W	=	resultant velocity
W_0	=	geometric resultant velocity
V	=	vertical velocity
n, N	=	revolutions per second and r.p.m., respectively
Γ	=	circulation
K	=	Goldstein circulation coefficient
L	=	lift
D	=	drag
T	=	thrust
Q	=	torque
P, hp.	=	power, horsepower
I_P, I_T	=	integrating coefficients for power and thrust distribution curves, respectively. Assumption is made that $I_P = I_T$
α	=	angle of attack for infinite aspect ratio
β	=	inflow angle
φ_0	=	geometric angle of advance
φ	=	geometric angle plus inflow
ϵ	=	true helix in wake, assumed equal to φ
θ	=	section blade angle
κ	=	Goldstein inflow factor
τ	=	ratio of $[(\kappa - z \text{ b'ades})/(\kappa - y \text{ blades})]_{0.75}$
ρ, ρ_0	=	air density and for standard, respectively
η	=	figure of merit
x	=	r/R
σ	=	solidity $= Bb/2\pi r$
C_L	=	$dL/(\rho W^2 b\, dr/2)$
C_D	=	$dD/(\rho W^2 b\, dr/2)$
C_T	=	$T/\rho n^2 D^4$
C_P	=	$P/\rho n^3 D^5$
C_Q	=	$Q/\rho n^2 D^5$

THE THEORY AND ITS FUNDAMENTAL EQUATIONS

THE AERODYNAMICS of the helicopter when viewed in all conditions of flight presents a maze of problems and a fruitful field for theoretic development.

Most notable contributions have been made by Glauert,[1] Knight,[2] Sissingh,[3] and many others, all of their works reaching toward the limit of practical solution in view of the prohibitive and laborious mathematics involved. However, as theory accompanies the progress of the helicopter itself, new methods of aerodynamic development will undoubtedly be set forth.

There are many published reports on the Goldstein vortex theory treating both the theoretic concepts and the means for practical use. Some of these reports, including Goldstein's original work, are listed[4, 5, 6, 7]. However, they have dealt particularly

Presented at the Rotating Wing Aircraft Session, Eleventh Annual Meeting, I.A.S., New York, January 25–29, 1943.

* Aerodynamicist, Hamilton Standard Propellers Division.

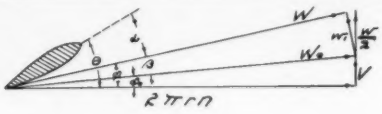

FIG 1.

with application to aircraft propellers. The author therefore takes this opportunity to introduce the theory to those in the rotary wing field who have not as yet become acquainted with the Goldstein theory.

The theory lends itself to immediate application at the hovering flight and vertical climb conditions. It is felt that improved precision in evaluating relative rotor performance will be possible and that aerodynamic design criteria may be established.

Heretofore, certain basic simplifications were essential for the application of the original vortex theory to helicopter performance; i.e., the assumptions were made that the circulation distribution was constant or varied uniformly with the radius, that the number of blades was infinite, and that rotational and radial components of velocity could be neglected. Although tests and classic studies of airplane propellers have indicated relative insensitivity of efficiency and static thrust to rather wide variations in radial thrust distributions for normal disc loadings, closer observation will show that at disc loadings equivalent to those of conventional rotors the efficiency sensitivity to thrust distribution becomes more pronounced.

Contrary to the foregoing assumptions, the Goldstein theory offers a solution for all of the named assumptions and, by application of the Betz criterion for optimum propellers, can be utilized to calculate optimum load distributions along with the plan forms and pitch distributions required for those conditions.

Goldstein[6] treated the pure hydrodynamic problem of the potential flow of fluid in space surrounding a set of equispaced coaxial helicoids of infinite length but of a finite radius and moving axially with a uniform velocity, the fluid being a rest at infinity. Betz[7] had previously shown that for propellers of minimum induced loss, $d\Gamma/dr$ is equal to one-half the discontinuity of potential across such surfaces, the number of helicoids corresponding to the number of blades.

Goldstein chose to define the circulation in terms of a nondimensional coefficient K.

$$\Gamma = Kw\ 2\pi r \tan \epsilon/B$$

Numerical values for K may be found in references 4, 5, and 6.

Lock[4] has shown that the fundamental expressions for axial and rotational velocity components of the elementary vortex theory are equivalent to those derived from Goldstein's work except for the factor κ ($\kappa = K/\cos^2 \epsilon$).

Values for κ have been redrawn from reference 5 with added interpolation for the 6-blade case. They are

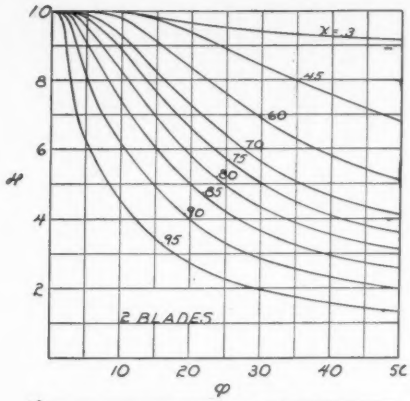

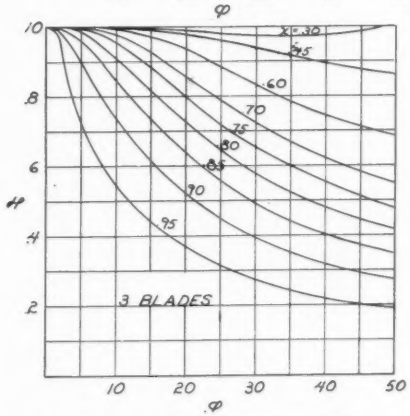

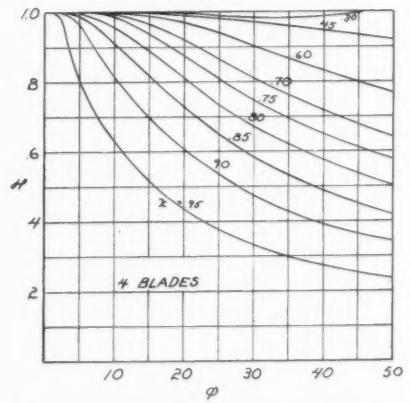

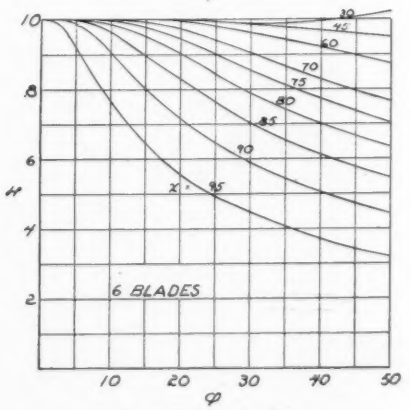

FIGS. 2a, 2b, 2c, 2d.

shown for 2, 3, 4, and 6 blades in Figs. 2a, 2b, 2c, and 2d.

Since radial independence has been proved, the resultant induced velocity may be expressed as,

$$w_1 = \frac{B\Gamma}{4\pi r \sin\varphi\kappa} \text{ (see Fig. 1)}$$

Reiterating the well-known equations,

$$dL/dr = \rho W\Gamma = \rho W^2 C_L b/2$$

Then:

$$w_1 = BbWC_L/8\pi r \sin\varphi\kappa$$

which reduces to

$$\sigma C_L = 4 \tan\beta \sin\varphi\kappa \qquad (1)$$

The effect of the profile drag on the induced velocity is purely secondary and has therefore been justifiably neglected since the complexity of including this variable in calculations would not be compensated for by improved accuracy. Furthermore, practical application of the theory to propeller problems has proved secondary effects to be unimportant below the stall.

The equations for elemental thrust and torque may be derived from the simple resolution of the lift and drag forces at each element. Transferring these to coefficient form, the expressions are:

$$\frac{dC_T}{dx} = \left(\frac{\pi^3}{4}\right)\sigma C_L x^3 \left(\frac{\cos^2\beta}{\cos^2\varphi_0}\right)\cos\varphi\left(1 - \tan\varphi\,\frac{C_D}{C_L}\right) \qquad (2)$$

$$\frac{dC_P}{dx} = \left(\frac{\pi^4}{4}\right)\sigma C_L x^4 \left(\frac{\cos^2\beta}{\cos^2\varphi_0}\right)\sin\varphi\left(1 + \cot\varphi\,\frac{C_D}{C_L}\right) \qquad (3)$$

When the blade angle is known for each element, it is obvious that the lift coefficient satisfying the theoretic expression for inflow must correspond to the lift coefficient consistent with infinite aspect ratio airfoil data for the particular section at the angle of attack $\alpha = \theta - \varphi$. Thus a precise analysis requires that a method of interpolation be used; for example, having assumed a β, the theoretic C_L may be readily calculated using Eq. (1) for a given section. The C_L from airfoil data is also known; hence the two must be made to coincide. The majority of theoretic papers on helicopter performance have chosen to establish the relation $C_L = K\alpha$, eliminating the necessity of interpolation. This leads to inaccuracies upon approaching the stall; whereas suitable airfoil data may be applied to special cases even beyond the stall and may serve to predict more precisely plan-form and blade width limitations at severe loading conditions.

Integration of the dC_T/dx vs. x and dC_P/dx vs. x curves yields the net C_T and C_P values. A procedure for calculation may now be established.

Select a series of r/R stations for analysis; the particular known quantities may then be θ, b/D, h/b, the vertical velocity, the r.p.m., and rotor diameter. For hovering, $\varphi_0 = 0$ and $\varphi = \beta$, while at other conditions $\varphi_0 = \tan^{-1}(V/2\pi rn)$:

(1) Assume β.

(2) Then $\beta + \varphi_0 = \varphi = \theta - \alpha$.

(3) Calculate $C_L = 4 \tan\beta \sin\varphi\kappa/\sigma$.

(4) From the α in step (2) read C_L from Fig. 3. Compare the calculated C_L to the airfoil C_L. If necessary, assume another β until the two values reasonably coincide.

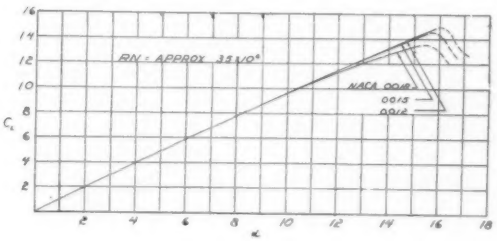

FIG. 3.

(5) Tabulate the proper C_D/C_L, selected from Fig. 4.

(6) Calculate

$$\frac{dC_T}{dx} = \left(\frac{\pi^3}{4}\right)x^3\sigma C_L\left(\frac{\cos^2\beta}{\cos^2\varphi_0}\right)\cos\varphi\left(1 - \tan\varphi\frac{C_D}{C_L}\right)$$

$$\frac{dC_P}{dx} = \left(\frac{\pi^4}{4}\right)x^4\sigma C_L\left(\frac{\cos^2\beta}{\cos^2\varphi_0}\right)\sin\varphi\left(1 + \cot\varphi\frac{C_D}{C_L}\right)$$

(7) Plot the results against x and integrate for C_T and C_P.

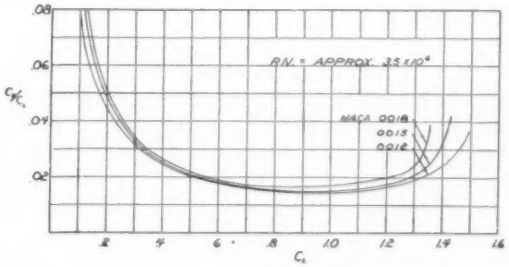

FIG. 4.

To analyze a rotor for a known C_P at the start, several approaches are possible. One would be to select at least two values for θ at the representative $0.75R$ station, calculate C_T and C_P accordingly, and plot the net results as desired.

Despite the fact that the general analysis does not deal with a rotor of optimum design wherein the results of Goldstein would rigidly apply, it is felt that application of κ to any circulation distribution represents a marked improvement over the original vortex theory.

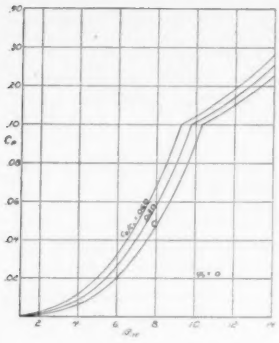

FIG. 5a.

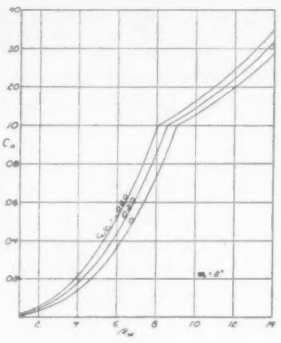

FIG. 5b.

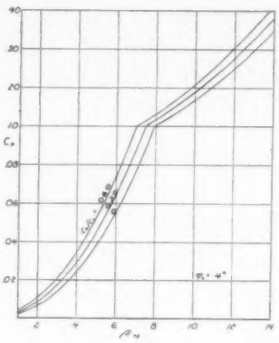

FIG. 5c.

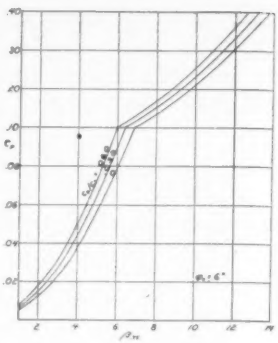

FIG. 5d.

Actual calculation may be greatly simplified by presenting portions of the equations as charts. For example, a graph can be made of Eq. (1), $\sigma C_L/\kappa$ may be plotted against β with parameters of φ_0 or V/nr. The quantity of $(\pi^3/4)\sigma C_L x^3(\cos^2 \beta/\cos^2 \varphi_0)$ may be factored from Eqs. (2) and (3). Substituting from Eq. (1), the quantity becomes $\pi^3 \tan \beta \sin \varphi \kappa x^3 (\cos^2 \beta/\cos^2 \varphi_0)$, which may be plotted as desired. The three equations thus lend themselves to a wide variety of structures consisting of charts, tables, etc., or other forms convenient for any type of application.

Although quite laborious, a complete analysis by longhand methods is justified for many types of detailed studies. For example, the previously mentioned effects of thrust distribution upon rotor efficiency may be studied along with the relative contribution of each section to the overall performance. The results so derived, when used in conjunction with momentum considerations, may further be employed to estimate the aerodynamic effects of the rotor slipstream upon the aircraft fuselage and supporting members.

Optimum Rotor Criteria

Optimum load distributions constitute an interesting field for theoretic study as well as a general guiding influence on the overall rotor design. In terms of the system described, an optimum distribution requires that the axial velocity, w, of the helicoid be constant.

This at once establishes the β distribution for a particular power coefficient and a given number of blades. It is then possible to compute the $(b/D)C_L$ at a series of radiuses or r/R stations.

As an application of the theory to practical considerations, optimum design criteria will be derived for the hovering flight conditions. A study has been prepared involving a series of calculations to find the $(b/D)C_L$ distribution for 2-, 3-, 4-, and 6-blade rotors' at typical power coefficients. The effects of varying the power absorption was slight, making possible the selection of a mean curve for each number of blades case. The family of mean curves thus found are shown in Fig. 10 plotted in ratio form. Observation will show that the load distribution shifts toward the tip with an increasing number of blades, the trend reflecting the use of κ since the κ curves approach 1.0 with the increasing number of blades.

A further significant trend is that of the increasing $(b/D)C_L$ with decreasing x. In the hovering condition the curves approach infinity while at any positive vertical velocity they swing back down to zero. However, in any case, sections inboard of $x \doteq 0.3$ contribute a negligible amount to the overall rotor performance and are, therefore, relatively unimportant. Considering then the sections from $x = 0.3$ to the tip, the optimum distributions require a marked taper in $(b/D)C_L$.

Optimum Blade Design

Optimum blade design is of pertinent interest and will, therefore, be discussed briefly.

In the next section it will be shown that a $[(b/D)C_L]_{0.75}$ can be found for any particular power coefficient and number of blades through the use of Figs. 5, 6, 7, and 2. Having established the distribution of $(b/D)C_L$ from Fig. 10, it is possible to attain this distribution by an infinite number of combinations of plan form and pitch distribution simply by arbitrary selection of either of the variables. Although Fig. 10 is rigidly applicable only for hovering analyses, it is quite reasonable to utilize the curves for cases at small $\varphi_{0.75}$ angles.

Inclusion of profile drag characteristics in performance calculations at once greatly restricts the range of C_L permissible for minimum profile power loss, therein establishing the limits of the C_L distribution. The minimum profile power loss will not necessarily occur at the minimum C_D of the section but near the minimum C_D/C_L. However, in selecting a rotor plan form to be used over a range of conditions the logical selection of C_L is one compromising minimum profile loss over the operating range with blade width, weight, section characteristics, and so on. If then a compromise C_L is selected at each station, the rotor pitch distribution and plan form become fixed.

In the broad picture of overall helicopter performance the designer is confronted with the problem of making the best all-around compromise so as to main-

TABLE 1
Values of C_P

C_D/C_L	0	0.01	0.02	0.03	0.045	0.060
β			$\varphi_0 = 0$			
2	0.000782	0.001008	0.001232	0.001456	0.001794	0.002126
4	0.00618	0.00706	0.00794	0.00884	0.01020	0.01152
6	0.0206	0.02258	0.02456	0.02648	0.02940	0.03238
8	0.0476	0.0510	0.0544	0.0578	0.0628	0.0680
10	0.0902	0.0954	0.1006	0.1058	0.1132	0.1210
12	0.1502	0.1576	0.1644	0.1710	0.1820	0.1928
14	0.2276	0.2368	0.2454	0.2548	0.2688	0.2820
			$\varphi_0 = 2.0°$			
2	0.00312	0.00357	0.00402	0.00446	0.00513	0.00580
4	0.0318	0.01512	0.01644	0.01774	0.01970	0.02166
6	0.0362	0.03876	0.0413	0.0438	0.0477	0.0516
8	0.0728	0.0770	0.0812	0.0854	0.0916	0.0978
10	0.1266	0.1326	0.1386	0.1442	0.1534	0.1626
12	0.1980	0.2060	0.2134	0.2216	0.2340	0.2454
14	0.2858	0.2960	0.3060	0.3160	0.3306	0.346
			$\varphi_0 = 4°$			
2	0.00696	0.00762	0.00828	0.00894	0.00992	0.01092
4	0.0242	0.02594	0.02764	0.02936	0.03192	0.03454
6	0.0552	0.0584	0.0616	0.0647	0.0694	0.0740
8	0.1022	0.1070	0.1120	0.1162	0.1238	0.1312
10	0.1668	0.1736	0.1800	0.1868	0.1970	0.2068
12	0.2486	0.2574	0.2664	0.2752	0.2880	0.3012
14	0.3468	0.3580	0.3680	0.3796	0.3950	0.4110
			$\varphi_0 = 6°$			
2	0.01228	0.01314	0.0140	0.01488	0.01618	0.01750
4	0.0372	0.03932	0.0414	0.04350	0.04670	0.04990
6	0.0778	0.0814	0.0852	0.0886	0.0942	0.0998
8	0.1348	0.1404	0.1454	0.1510	0.1594	0.1672
10	0.2100	0.2176	0.2248	0.2324	0.3424	0.2542
12	0.3034	0.3130	0.3218	0.3318	0.3456	0.3590
14	0.410	0.421	0.4330	0.444	0.4610	0.478

tain a good rotor design for all aerodynamic conditions, along with the necessity of maintaining structural simplicity. General aerodynamic considerations show that an optimum blade design for hovering and vertical climb would conflict with the most desirable features for horizontal top speed and level flight and with rotors designed for autorotation. In level flight there is a reversed velocity field over a portion of the retreating blade. Although this region covers only a small portion of the radius, it would still require minimum loading over that region if optimum blade performance is to be attained. When a rotor is autorotating, the innermost stations of a blade are stalled, thereby reducing the r.p.m. somewhat for a given weight and rate of descent. Consequently, here again, a minimum of inboard loading would be preferred. Nevertheless, optimum design criteria are most desirable in planning the necessary compromise where emphasis may well be placed on some particular performance requirements.

In all considerations there is a definite limit to the theoretic means of calculating performance and still further to the theoretic development itself. Although autorotating blades have been substantially tested in view of the development of the autogiro, there is still practically no data available on power-driven rotors, particularly in forward flight conditions. It is appreciated that current helicopter developments involve such uncertain features as cyclic pitch control, coning angles, the blade designs, and other factors. Nevertheless, rotor performance is stable enough to warrant testing at a wide range of forward velocities. The opportunity is taken to urge the setting up of test programs by laboratories so that the meager tests available may be extended and so that data may be contributed where there is today no data at all.

SIMPLIFIED SYSTEM OF CALCULATION

Although the complete theory is useful in particular types of detailed aerodynamic study such as those just mentioned, it is often desirable to have a rapid method of performance calculation available for those types of analyses involving initial overall rotor design characteristics; e.g., rotor diameters, width ratios, operating r.p.m.'s, horsepowers necessary for a required thrust, etc.

Curves showing the variation of thrust plotted against these variables are therefore useful when used with structural considerations as a basis for the selection of a rotor and the operating conditions for its design.

Still further performance calculations may be conducted for established rotor designs.

Where the plan form and pitch distribution are known or may be estimated, it is possible to select a suitable integrating factor and proceed to analyze only a representative station at, say, $0.75R$.

The power coefficient may be written:

$$C_P = \left(\frac{\pi^4}{2}\right) x^4 \left(\frac{\sin 2\beta \sin^2 \varphi \kappa}{\cos^2 \varphi_0}\right) I_P \left(1 + \frac{C_D}{C_L} \cot \varphi\right) \tag{4}$$

For normal values of φ_0 and for an $I_P = 0.6$, the equation reduces to:

$$C_P = 9.22 \left(\frac{\sin 2\beta \sin^2 \varphi \kappa}{\cos^2 \varphi_0}\right)\left(1 + \frac{C_D}{C_L} \cot \varphi\right)$$

and is plotted in Figs. 5a, 5b, 5c, 5d, for φ_0 values of 0, 2°, 4°, 6°. The values used in drawing the curves are tabulated in Table 1. Conveniently, there is little variation in C_D/C_L with increasing C_L below the stall, so that 0.015 is a good estimate where optimum performance is being considered.

For comparative studies of rotors over a wide range of the principal variables, the assumption of a constant integrading factor equal to 0.60 is quite reasonable. However, consideration of actual magnitudes should be conducted with caution, since the particular loading characteristics may render an I_P value anywhere between the extremes of 0.50 and 0.65. A flat pitch, rectangular plan-form blade would have an I_P of approximately 0.57; whereas an optimum loading at a normal power absorption would give an I_P of approximately 0.60. Hence, in the derivation the optimum I_P was used.

Because of the presence of κ, provision must be made to include the effect of number of blades on C_P. Figs. 5a, 5b, 5c, and 5d and Table 1 have been computed

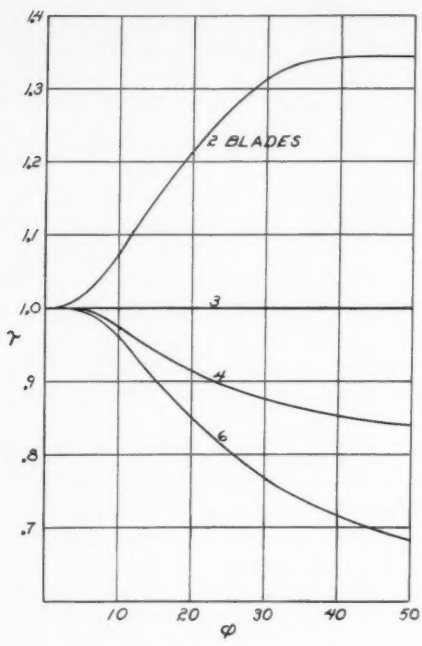

FIG. 6.

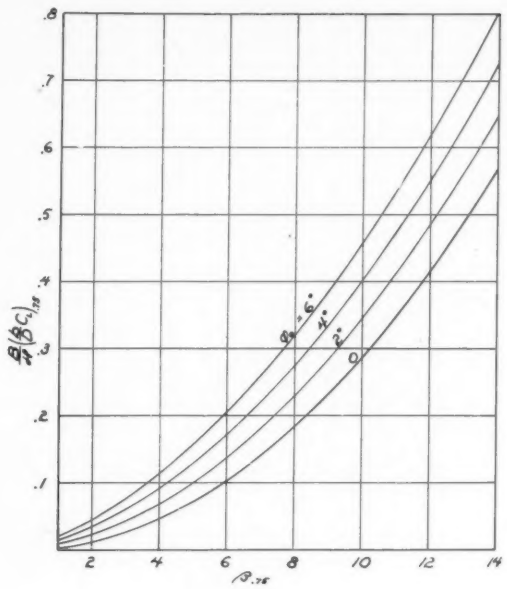

FIG. 7.

using the κ corresponding to three blades. It is reasonable to assume that C_P is a function of β, whereby it is possible to obtain the β for y blades by simply multiplying the β for three blades by the ratio of $\kappa - z$ blades/$\kappa - y$ blades. This ratio has been named τ and is shown in Fig. 6.

In seeking a relationship between β and the blade $(b/D)C_L$ ratio, application is made of the equation:

$$\sigma C_L/\kappa = 4 \tan \beta \sin \varphi$$

or

$$\frac{B}{\kappa_{0.75}}\left(\frac{b}{D} C_L\right)_{0.75} = 9.43 \tan \beta \sin \varphi \qquad (1a)$$

which is plotted in Fig. 7 and tabulated in Table 2. The relation $\varphi_0 = \tan^{-1}(V/2\pi rn)$ may be simplified to $\varphi_{0.75} = 729\ (V/NR)$ degrees.

Combining Eqs. (2) and (3), the ratio of thrust and power coefficients is

$$\frac{C_T}{C_P} = \left(\frac{\cot \varphi}{\pi x}\right)\left(1 - \frac{C_D}{C_L} \tan \varphi\right) \Big/ \left(1 + \frac{C_D}{C_L} \cot \varphi\right)$$

as is shown in Fig. 8 with the accompanying values in Table 3.

In conjunction with the use of the above, additional charts have been prepared showing airfoil characteristics. It is essential, in view of torsional oscillation, to incorporate airfoils of practically zero pitching moment such as those reported in references 8 and 9. For this study, the N.A.C.A. 00 series has been selected as representative. Fig. 3 shows the lift variation with

TABLE 2

Values of $(B/\kappa)[(b/D)C_L]_{0.75}$

φ_0	0°	2°	4°	6°
β				
2	0.01147	0.0229	0.0344	0.0458
4	0.0459	0.0687	0.0915	0.1142
6	0.1036	0.1380	0.1719	0.2055
8	0.1842	0.230	0.275	0.320
10	0.2885	0.3455	0.401	0.457
12	0.416	0.485	0.551	0.619
14	0.567	0.647	0.725	0.802

angle of attack for infinite aspect ratio, while Fig. 4 shows the change in C_D/C_L with increasing C_L. A most important factor is that of Reynolds number; the rotor tips may be up around 3,500,000, which value decreases practically linearly with decreasing radius. In a precise elemental analysis of the type described in the previous section, airfoil data for the appropriate Reynolds numbers would be preferred. However, for the simplified system, the data corresponding to a RN of 3,500,000 should be satisfactory although somewhat optimistic.

The momentum theory has long been applied as a means of predicting the ideal limit of thrust attainable for a given diameter and horsepower. Restating the hovering derivation for completeness:

If $V_s/2$ is the slipstream velocity at the rotor,

$$T = \rho\pi R^2 V_s^2/2$$

and for 100 per cent conversion of energy into useful thrust

$$\text{hp.} = (\rho\pi/4)R^2 (V_s^3/550)$$

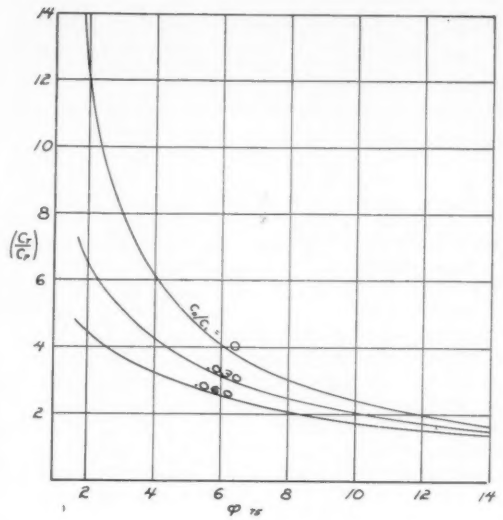

FIG. 8

TABLE 3
Values of C_T/C_P

C_D/C_L	0.0	0.01	0.02	0.03	0.045	0.06
φ						
2.0	12.12	9.47	7.74	6.55	5.31	4.47
3.0	8.12	6.80	5.87	5.15	4.26	3.77
4.0	6.07	5.32	4.72	4.25	3.685	3.26
6.0	4.05	3.69	3.39	3.145	2.815	2.56
8.0	3.02	2.82	2.64	2.49	2.275	2.10
10.0	2.415	2.27	2.155	2.045	1.902	1.778
12.0	1.999	1.90	1.812	1.743	1.580	1.54
14.0	1.708	1.63	1.569	1.510	1.425	1.357

Solving to eliminate V_s,

$$T = 10.4 = 2[(D)(\text{hp.})]^{2/3} \ (\rho/\rho_0)^{1/3}$$

The equation is plotted in Fig. 9 for the case at sea level.

Curves are drawn for various diameters showing ideal thrust in lbs. vs. hp.

A figure of merit may then be calculated as the ratio of actual thrust to the ideal thrust.

A simple analysis method may now be systemized and successive steps established. The method will be illustrated in a form suitable for obtaining the rotor thrust, having known or assumed the other major variables. The flexibility of the system, however, permits solution for any desired parameter just as easily by merely setting up the procedure in a different order.

The quantities that must be known or assumed in computing the thrust are: N, hp., altitude, V, diameter, and number of blades.

(1) Calculate $C_P = (10^{11})$ (hp.) $(\rho_0/\rho)/2.0\ N^3\ D^5$.

(2) Calculate $\varphi_{0.75} = 729\ (V/NR)$.

(3) Figs. 5a, 5b, 5c, 5d, and 6 may be used to get β.

(4) Obtain $[(b/D)C_L]_{0.75}$ from Figs. 2 and 7. The

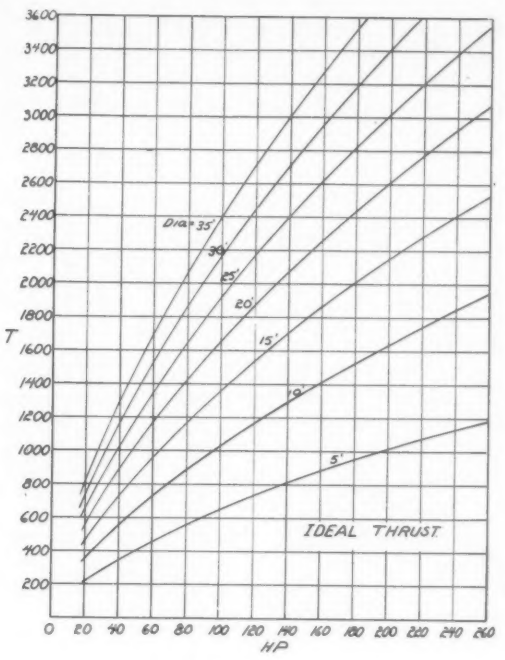

FIG. 9.

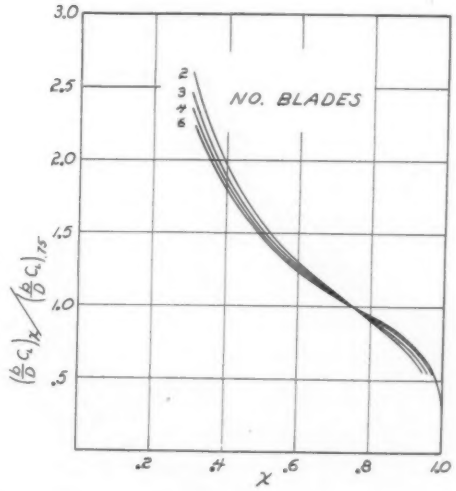

FIG. 10.

C_L may be simply calculated if the $(b/D)_{0.75}$ is fixed or arbitrarily, the $(b/D)_{0.75}$ may be selected for any desirable compromise C_L.

(5) From Fig. 8, tabulate C_T/C_P, which renders C_T if desired.

(6) The thrust is then: $T = (C_T/C_P)/(\text{hp.}/ND) \times 33{,}000$.

(7) Fig. 9 gives the ideal thrust whereupon the ratio of the two, η, is the figure of merit.

In making a study for the initial selection of the major variables listed as known or assumed, a convenient procedure would be to calculate performance curves bracketing the range of the variable or variables in

question. For example, performance curves may be calculated to determine thrust variation with r.p.m., hp., diameter, altitude, blade width, etc., or relative figure of merit curves versus r.p.m., hp., blade width, etc.

The interrelationship of such factors is subject matter for a complete paper in itself, particularly with the inclusion of the physical aspects of the rotor design such as weight, stresses, vibration, practical limitations on diameter, section thickness, etc.

References

[1] Glauert, H., *On the Vertical Ascent of Helicopter*, R. & M. No. 1132, 1927–1928.

[2] Knight, M., and Hefner, R., *Static Thrust Analysis of the Lifting Airscrew*, N.A.C.A. T.N. No. 626, December, 1937.

[3] Sissingh, G., *Contributions to the Aerodynamics of Rotating-Wing Aircraft*, N.A.C.A. T.M. No. 921, 1939; *Contribution to the Aerodynamics of Rotating-Wing Aircraft*, Part II, N.A.C.A. T.M. No. 990, 1941.

[4] Lock, C. N. H., *Application of Goldstein's Airscrew Theory to Design*, R. &. M. No. 1377, November, 1930.

[5] Lock, C. N. H., *Graphical Method of Calculating Performance of Airscrew*, R. & M. No. 1675, 1935.

[6] Goldstein, S., *On the Vortex Theory of Screw Propellers*, Proc. Royal Society of London, Vol. A 123, No. A 792, pp. 440–465, April, 1929.

[7] Betz, A.,"Schrauben propellermit geringstem Energieverlust," in *Vier Ablandungen zur Hydrodynamik und Aerodynamik* by L. Prandtl and A. Betz, pp. 68–92; Göttingen, 1927.

[8] Jacobs, Eastman N., and Abbott, Ira H., *Airfoil Section Data Obtained in the NACA Variable-Density Tunnel As Affected by Support Interference and Other Corrections*, N.A.C.A. T.R. No. 669, 1939.

[9] Jacobs, Eastman N., and Sherman, Albert, *Airfoil Section Characteristics as Affected by Variations of the Reynolds Number*, N.A.C.A. T.R. No. 586, 1937.

Letter to the Editor

Dear Sir:

Since the publication of my paper, ("Space Limitations and Optimum Spring Design," Journal of the Aeronautical Sciences, Vol. 10, No. 2, pp. 51–57, February, 1943) Example 3 on the minimum weight of an extension spring has been revised to apply to a more general problem—i.e., for a given load P_2, the lowest weight spring will be found by making the load $P_{max.}$ approximately equal to $1.9P_2$. If space limitations make this impossible, Eq. (4), page 53, will give the minimum weight. A more complete discussion of this problem including the effects of inactive spring material is given in the paper described below.

As the above paper was limited to only a few of the problems that can be solved by an optimum design method, many useful results and practical methods of application were necessarily omitted. For those interested in the subject, a more comprehensive discussion of optimum spring design, including the effects of initial tension, helix angle, weight considerations, etc., with the corresponding graphs and alignment charts for the three types of springs (extension, compression, and torsion), may be obtained from the Paul Kollsman Library of the Institute of the Aeronautical Sciences (title—"General Theory of Optimum Spring Design and Common Applications").

Richard H. Carter
Structural Research Engineer
United Aircraft Corporation

Problems of Routine Propeller Balancing

JERE T. FARRAH*
American Airlines, Inc.

SUMMARY

One of the most obvious sources of vibration in an airplane is the engine-propeller combination. For greater passenger and crew comfort plus reduced maintenance, vibration must be kept to a minimum.

All types of vibration equipment depend upon mechanical forced vibrations in some structure, which is caused to vibrate by the engine-propeller combinations. The amplitude of vibration may be determined either electrically or mechanically, and the direction of the unbalance may be determined either by a strobotron, electrically, or by the addition of added unbalance to the various propeller blades.

Propellers are usually balanced upon the airplane but have been successfully balanced several times upon a test stand.

Small factors affect the propeller balance. However, large factors such as the loss of a tip of a propeller have gone unnoticed.

It is recommended that propeller manufacturers should build into the propeller a device for balancing propellers. Propeller balancing equipment should be further developed to be accurate, simple, and easy to use.

REASONS FOR PROPELLER BALANCING

AN AIRPLANE for passenger transport use must be smooth. No matter how safe the operations of an air line may be, a passenger is poorly impressed if the plane in which he rides is noisy or has excess vibration. Passenger comfort is naturally increased by reducing all vibrations and noise to a minimum. In addition to passenger comfort, the crew must also be considered, and it is a well-established fact that crew fatigue is influenced considerably both by noise and vibrations. The airplane and its many mechanical accessories are less affected by fatigue failures and general loosening up if vibration is kept to a minimum. A considerable percentage of maintenance labor and costs is due directly to vibration. Accessories, brackets, engine mounts, and heaters are all adversely affected by constant vibration. Elimination of such vibration would reduce the maintenance, and at the same time fewer mechanical failures mean greater safety.

Causes of Vibration

One of the most obvious causes of vibration is the engine-propeller combination. In some airplanes the effects of engine-propeller unbalance are much more noticeable than in others. The propeller gear ratio has a great influence on propeller vibration. In the 3:2 gear ratio, the engine and propeller are in the same phase with respect to each other every three revolutions. In the 16:11, however, the engine and propeller are in the same phase only every 16 revolutions. In the case of the 3:2 ratio, vibrations repeat often enough to build up to comparatively large magnitudes. In the 16:11 ratio, however, the vibrations of the engine and propeller are out of phase, in varying degrees, enough so that amplitudes do not become large. The same general considerations apply to engines having a 2:1 ratio or a 16:9 ratio, the vibrations becoming a problem in the case of the 2:1 gear ratio. Thus there has developed a feeling that propeller balancing is necessary in some planes and unnecessary in others. Actually, all engine-propeller combinations need to be dynamically and aerodynamically balanced. Unbalance exists in the engine-propeller combinations in all airplanes but does not build up to large amplitudes in all cases. The fact that the natural frequency of vibration varies from one airplane to another and may or may not coincide with the critical frequency of the propeller is another important factor affecting propeller balancing requirements.

TYPES OF EQUIPMENT

There are numerous types of apparatus for propeller balancing—some simple, some complicated—the cost of the equipment accordingly varying from a few cents to hundreds of dollars. All types have one fundamental in common, however. All depend upon mechanical, forced vibrations in some object, usually a part of the airplane structure. Recent tests, however, have indicated that balancing may be accomplished on the test stand after the engine has been run-in following an overhaul, so that the balancing in that case is entirely independent of the airplane structure.

The amount of unbalance is determined in two fundamental ways. The most common method is by observing the amplitude of forced vibrations of some object, either a part of the airplane or incorporated in an instrument held securely to a part of the airplane.

Methods of Balancing

The standard method of balancing propellers on air-line DC-3's is by observing the amplitude of vibrations of the control column, which happens to have a natural frequency of vibration approximately the same as the critical frequency of the propeller. A method that has met with success in other types of aircraft consists of a reed having a varied free length.

Presented at the Power Plants and Propellers Session, Eleventh Annual Meeting, I.A.S., New York, January 25–29, 1943.

* Chief Flight Analyst.

The free length is adjusted so that the natural frequency of the reed is the same as the critical frequency of the propeller. The structure supporting the reed is then clamped on or held against some part of the airplane vibrating in resonance with the propeller. The amplitude of the vibration of the reed is then observed and is a measure of the propeller unbalance.

The amount of unbalance is electrically determined in other equipment. The equipment consists essentially of a coil (Fig. 1) that moves in a magnetic field. The output of the coil is proportional both to the amplitude and frequency of the vibration of the part to which the vibration pickup is attached. The output of the coil is determined by a suitable meter.

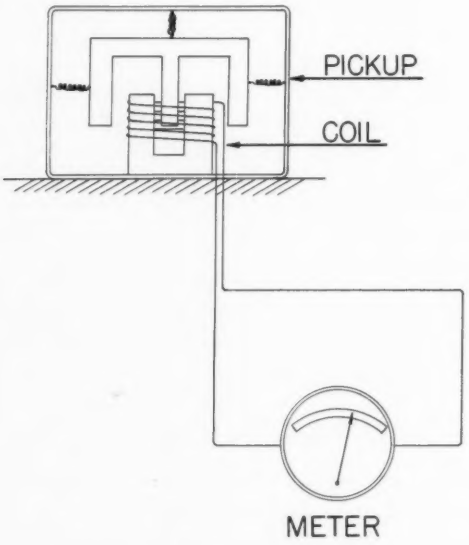

FIG. 1. Basic electrical vibration pickup.

A more advanced version of the above-mentioned equipment combines the output of the vibration pickup with the current from a generator running at propeller speed (Fig. 2). The vibration pickup is made to produce a current having a sine wave. The generator produces a three-phase alternating current. This is led to a transformer having a three-phase primary circuit and a single-phase secondary. The secondary is movable through 360°. Thus there is produced a second current having a variable-phase angle and also having a sine wave. The current from the pickup and that from the secondary of the transformer or phase shifter are led to a wattmeter. The phase angle of the secondary current is changed until the reading of the wattmeter is zero. At this point the phases of the current from the vibration pickup and the secondary are 90° apart (Fig. 3A). Shifting the phase angle of the secondary 90° (Fig. 3B) puts the two currents in phase and the meter reading is then a measure of the amount of vibration. The result is a vector having an angular position determined from the phase shifter and magnitude as read from the meter. The blade is run bare and a reading of angle and magnitude (Fig. 4) is taken. Then an unbalance of known magnitude is added to one of the blades. A second reading is taken, and the unbalance is then the resultant of the bare propeller's original unbalance and the added unbalance. The vector difference of the two readings is caused by the added unbalance. Since the direction and magnitude of the added unbalance are known (it being attached to one of the blades), the direction with respect to the propeller and the amount of the original unbalance can be determined, and suitable counter weights can be added to the hub bolts to compensate for the unbalance.

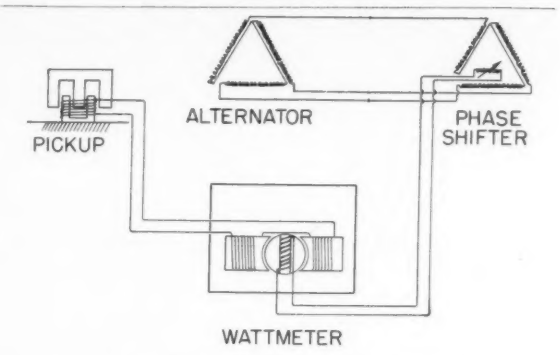

FIG. 2. Vibration pickup having means of determining both amount and direction of unbalance.

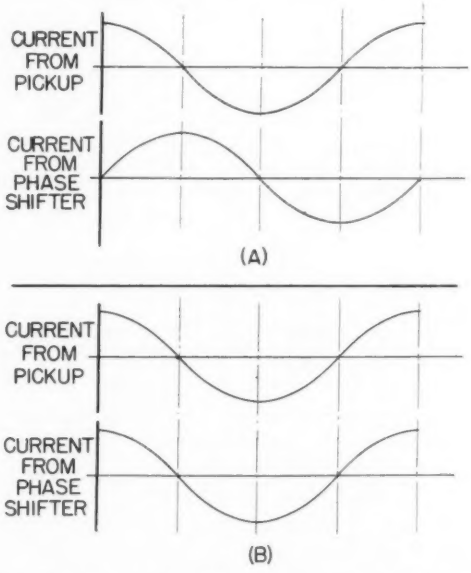

FIG. 3. Relative phase angles for maximum and zero meter readings. A = zero meter reading; B = maximum meter reading.

Direction of Unbalance

The direction of the unbalance is determined in other equipment by means of a strobotron. The strobotron is caused to light when the unbalance is in a definite

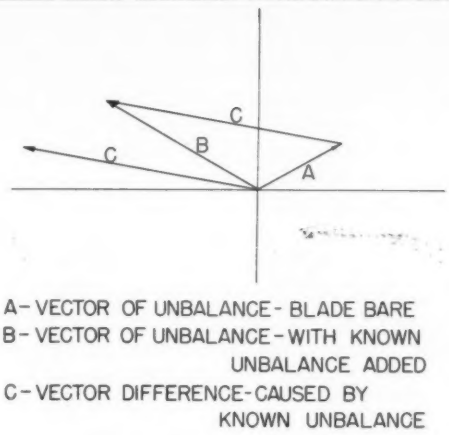
C
B
C
A
A- VECTOR OF UNBALANCE - BLADE BARE
B- VECTOR OF UNBALANCE - WITH KNOWN UNBALANCE ADDED
C- VECTOR DIFFERENCE - CAUSED BY KNOWN UNBALANCE

FIG. 4. Vector solution for determining original unbalance by addition of one added unbalance of known magnitude and direction.

direction. Since the light then flashes at propeller speed, the propeller appears stationary. If the three blades are identified, the position of the unbalance can then be determined visually, knowing the direction of the unbalance when the light is caused to flash.

The direction of unbalance is most commonly determined by adding an unbalance to each of the blades successively. The reading that is a measure of the unbalance (measure by any of the methods mentioned above—i.e., by means of noting the amplitude of a vibrating member, either mechanically or electrically) is plotted in the direction of each blade (Fig. 5). The resultant of the vectors is a measure of the direction and amount of unbalance. This solution is not rigorously correct because the unbalance measured is actually the resultant of the original plus the added unbalance and, therefore, not necessarily in the direction of the blade to which it is added. The solution is accurate enough, however, so that usually a satisfactory balance can be achieved after two or three trials.

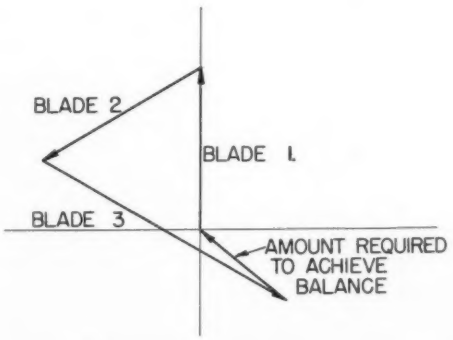

FIG. 5. Vector diagram to determine direction of original unbalance by adding unbalance to each blade successively. Amount of unbalance is determined by trial and error.

BALANCING PROPELLERS ON TEST STANDS

Propellers are nearly always balanced upon the airplane on which they are to be used. Research is now under way to develop a method of balancing engine-propeller combinations on the test stand. Several propellers have been successfully balanced on the test stand. Following the run-in, a flight propeller was mounted on the engine (Fig. 6). The propeller was balanced and was left on the engine, nothing being changed. The engine was then mounted in the airplane and the balance checked. No conclusive results have been reached using this method, but it is felt that this is a promising approach to the problem. Obvious savings in airplane time would result from having the propeller balanced when installed in the airplane.

FIG. 6. Picture of test stand set up for balancing flight propeller on the engine on the test stand following engine run-in.

Another advantage of balancing on the test stand is that wind and weather conditions are less severe than out in the open. Wind and gusts do occur in the test stand, but on the whole it is felt that conditions are much less severe.

Test stand conditions are not the same as in the plane. The vibrations caused by tips passing the fuselage and wing are missing on the stand, and the airflow behind the propeller is different. These effects appear small in magnitude, however, since propellers have been successfully balanced on the test stand in several cases.

The Hamilton Standard Propellers Division of the United Aircraft Corporation was interested to know the amount and direction of unbalance in a propeller when the propeller-engine combination had been balanced as accurately as possible on the airplane. A propeller was mounted on an engine on a DC-3 and

balanced as well as possible. The propeller was then removed and sent to Hamilton Standard where its unbalance was measured on their Gisholt Balancing Machine. The results were as follows:

Blade Angle (42-In. Station)	Static Unbalance	Dynamic Unbalance
17.2°	28.5 oz. in. at 154°	725 oz. in.^{2} at 314°
19 8°	32.5 oz. in. at 156°	700 oz. in.^{2} at 315°
23.9°	42.5 oz. in. at 134°	690 oz. in.^{2} at 325°

Blade No. 3 was located at 330° on the Balancing Machine Protractor.

Since the propeller-engine combination was originally balanced on the airplane, a large part of the unbalance as above tabulated is probably due to the engine and to aerodynamic unbalance caused by the airflow over the airplane.

Problems of Propeller Balancing

Propeller balancing is a strange problem. Extremely small things affect the balance. If a propeller dome is pulled and replaced as nearly as possible in the original position, the balance is sometimes changed. If a propeller is removed from an engine and replaced on the same spline, with the same position of the rear cone, the balance may be changed. If an accurate balance is to be achieved, the propeller must be changed from high to low pitch several times so that the oil in the dome is free from bubbles, etc. Small things have a seemingly large effect. On the other hand, a scheduled air liner hit an obstruction with the tip of a propeller when taxiing for a take-off. The tip of the propeller was sheared off but was not noticed. A normal run-up and take-off followed, and the unbalance was not noticed until the engine was throttled back for the next landing. In another case, the end of a rubber alcohol deicer shoe was lost from one blade. No undue vibration was observed. Numerous such incidents have occurred. How can such relatively large unbalances be barely noticed if at all when in the original unbalance, small washers weighing 0.133 oz. have a measurable effect when placed in hollow hub bolts? Of course, the natural frequencies of the various parts of the structure may not be in resonance in all cases. Is there a fundamental error in the analysis of the cause and effects of propeller vibrations?

One obvious discrepancy exists when the balancing weights are placed all in one plane. With a mass as large as an engine-propeller combination, it is difficult to believe that the resultant unbalance should be in one plane. It is more likely that a couple should be added to achieve a balance. A means of determining the magnitude and angular position of the couple should be developed, plus a means of adding a couple to the propeller.

The propeller manufacturers should build into the propeller a means for correcting unbalances that occur when the propeller is put into use. This should preferably be such that a couple could be added, weights being added to two planes. Whatever the means, it should be simple and easy to use when applied to routine servicing.

Much development remains to be done in balancing equipment. Balancing apparatus should be accurate, compact, easily set up, and such that the average line mechanic can easily use it and understand its underlying principles.

Much research remains to be done concerning propeller balancing. The possibilities of balancing propeller-engine combination on the test stand following the run-in must be further investigated. The fundamental problem must be carefully reviewed with special emphasis on developing a means of measuring an unbalanced couple, if there is such, and correcting for it accurately and quickly.

Design-Strengthened Materials

RICHARD S. SMITH* AND HAMILTON GRAY†

Rigid-Tex Corporation and New York University

SUMMARY

The purpose of this paper is to present pertinent design data and descriptive information on a process for increasing the strength-weight ratios of flat sheets of high-strength steel, aluminum alloy, and other metals.

Briefly, "design-strengthening," as the process is called, is accomplished by passing sheet and strip through specially prepared rolls that have, on their surfaces, a pattern that is transferred to either the top or bottom surface of the flat sheet or to both surfaces. The patterns are designed to improve such characteristics of the sheet—resistance to impact, stiffness, buckling strength, fatigue resistance, etc.—as may be dictated by the structural requirements.

Tables of properties of the several design-strengthened materials are presented. In these tables the properties of the original flat sheets are given for comparative purposes.

DESIGN-STRENGTHENING

A COMMON METHOD of strengthening flat sheet by *forming* is to corrugate it. Structural design engineers are familiar with the tremendous increase in buckling strength for carrying axial loads parallel to the corrugations and the increased rigidity and strength for carrying transverse loads. Corrugations, however, have the following inherent disadvantages:

(1) The strength of the sheet is increased in only one direction—parallel to the corrugations. The buckling strength and stiffness perpendicular to the corrugations are decreased.

(2) The weight per unit of projected area is greater for the corrugated sheet than for the flat sheet.

(3) The workability of corrugated sheet is limited.

From an engineering standpoint *design-strengthening* can be applied to strengthen the sheet in one direction without any loss in strength in a perpendicular direction, or it can be designed and applied to strengthen the sheet in two directions perpendicular to each other, thereby eliminating disadvantage (1) of the ordinary corrugation. Also the average or "weight" thickness of the design-strengthened sheet can be made equal to the thickness of the plain cold-reduced sheet, or it can be somewhat reduced by the design-strengthening process; thus the weight per unit of projected area remains the same as that of a plain sheet or is reduced, thereby eliminating disadvantage (2). The workability of design-strengthened sheets is not limited as in the case of corrugated sheets, since the former can be stamped, drawn, formed, roll formed, spot welded or seam welded, thereby eliminating disadvantage (3). If advantageous, depending on the application, design-strengthened sheets can be subjected to a degree of cold working in order to further improve certain strength characteristics, or they can be subjected to a negligible amount of cold working so as to not affect their workability or ductility.

It is obvious that the degree of design-strengthening may be regulated within certain limits (a) by the design of the pattern itself and (b) by its depth.

Figs. 1a, 1b, and 1c show samples of design-strengthened surfaces. The particular patterns in Fig. 1a are referred to as No. 1 WL, No. 2 WL and No. 5 WL. (WL designates wavy line pattern.) Three degrees of depth are shown, No. 1 WL being the minimum and No. 5 WL the maximum for this type of pattern. It is important to observe the decrease in weight below that of the flat sheet and the increase in overall thickness. This decrease in weight per unit of area and increase in overall thickness serve to increase the effective *EI* (the stiffness factor) of the sheet per unit of weight.

Fig. 2 shows an enlarged transverse cross section where the maximum overall thickness occurs in a No. 5 WL pattern. In this figure is illustrated the brief definition of design-strengthening—*the redistribution of metal in flat sheets for the purpose of obtaining maximum strength-weight ratios and maximum rigidity-weight ratios.*

An important point is that the *end use* determines the geometric shape and dimensions of the pattern. In other words, the design engineer can devise or select the optimum finish for each and every application of design-strengthened materials. Displacement of metal can be increased to gain maximum rigidity (resistance to bending), or it can be decreased to meet other requirements of the finished parts. The radiuses of the lobes in the pattern may be increased to improve transverse-bending fatigue-stress values, or they may be reduced to secure maximum flexural rigidity if the latter value is of greater importance in the part being designed. *Plain areas* can be incorporated in the pattern for riveting or seam welding or for other purposes.

TENSILE PROPERTIES

Table 1 shows the tensile properties of plain and design-strengthened flat sheets of stainless steel (17–7). Table 2 shows the tensile properties of plain and design-strengthened flat sheet of carbon steel (SAE 1010) and

Presented at the Materials Session, Eleventh Annual Meeting, I.Ae.S., New York, January 25–29, 1943.

* President.

† Consultant, College of Engineering.

balanced as well as possible. The propeller was then removed and sent to Hamilton Standard where its unbalance was measured on their Gisholt Balancing Machine. The results were as follows:

Blade Angle (42-In. Station)	Static Unbalance	Dynamic Unbalance
17.2°	28.5 oz. in. at 154°	725 oz. in.^{2} at 314°
19.8°	32.5 oz. in. at 156°	700 oz. in.^{2} at 315°
23.9°	42.5 oz. in. at 134°	690 oz. in.^{2} at 325°

Blade No. 3 was located at 330° on the Balancing Machine Protractor.

Since the propeller-engine combination was originally balanced on the airplane, a large part of the unbalance as above tabulated is probably due to the engine and to aerodynamic unbalance caused by the airflow over the airplane.

Problems of Propeller Balancing

Propeller balancing is a strange problem. Extremely small things affect the balance. If a propeller dome is pulled and replaced as nearly as possible in the original position, the balance is sometimes changed. If a propeller is removed from an engine and replaced on the same spline, with the same position of the rear cone, the balance may be changed. If an accurate balance is to be achieved, the propeller must be changed from high to low pitch several times so that the oil in the dome is free from bubbles, etc. Small things have a seemingly large effect. On the other hand, a scheduled air liner hit an obstruction with the tip of a propeller when taxiing for a take-off. The tip of the propeller was sheared off but was not noticed. A normal run-up and take-off followed, and the unbalance was not noticed until the engine was throttled back for the next landing. In another case, the end of a rubber alcohol deicer shoe was lost from one blade. No undue vibration was observed. Numerous such incidents have occurred. How can such relatively large unbalances be barely noticed if at all when in the original unbalance, small washers weighing 0.133 oz. have a measurable effect when placed in hollow hub bolts? Of course, the natural frequencies of the various parts of the structure may not be in resonance in all cases. Is there a fundamental error in the analysis of the cause and effects of propeller vibrations?

One obvious discrepancy exists when the balancing weights are placed all in one plane. With a mass as large as an engine-propeller combination, it is difficult to believe that the resultant unbalance should be in one plane. It is more likely that a couple should be added to achieve a balance. A means of determining the magnitude and angular position of the couple should be developed, plus a means of adding a couple to the propeller.

The propeller manufacturers should build into the propeller a means for correcting unbalances that occur when the propeller is put into use. This should preferably be such that a couple could be added, weights being added to two planes. Whatever the means, it should be simple and easy to use when applied to routine servicing.

Much development remains to be done in balancing equipment. Balancing apparatus should be accurate, compact, easily set up, and such that the average line mechanic can easily use it and understand its underlying principles.

Much research remains to be done concerning propeller balancing. The possibilities of balancing propeller-engine combination on the test stand following the run-in must be further investigated. The fundamental problem must be carefully reviewed with special emphasis on developing a means of measuring an unbalanced couple, if there is such, and correcting for it accurately and quickly.

Design-Strengthened Materials

RICHARD S. SMITH* AND HAMILTON GRAY†

Rigid-Tex Corporation and New York University

SUMMARY

The purpose of this paper is to present pertinent design data and descriptive information on a process for increasing the strength-weight ratios of flat sheets of high-strength steel, aluminum alloy, and other metals.

Briefly, "design-strengthening," as the process is called, is accomplished by passing sheet and strip through specially prepared rolls that have, on their surfaces, a pattern that is transferred to either the top or bottom surface of the flat sheet or to both surfaces. The patterns are designed to improve such characteristics of the sheet—resistance to impact, stiffness, buckling strength, fatigue resistance, etc.—as may be dictated by the structural requirements.

Tables of properties of the several design-strengthened materials are presented. In these tables the properties of the original flat sheets are given for comparative purposes.

DESIGN-STRENGTHENING

A COMMON METHOD of strengthening flat sheet by *forming* is to corrugate it. Structural design engineers are familiar with the tremendous increase in buckling strength for carrying axial loads parallel to the corrugations and the increased rigidity and strength for carrying transverse loads. Corrugations, however, have the following inherent disadvantages:

(1) The strength of the sheet is increased in only one direction—parallel to the corrugations. The buckling strength and stiffness perpendicular to the corrugations are decreased.

(2) The weight per unit of projected area is greater for the corrugated sheet than for the flat sheet.

(3) The workability of corrugated sheet is limited.

From an engineering standpoint *design-strengthening* can be applied to strengthen the sheet in one direction without any loss in strength in a perpendicular direction, or it can be designed and applied to strengthen the sheet in two directions perpendicular to each other, thereby eliminating disadvantage (1) of the ordinary corrugation. Also the average or "weight" thickness of the design-strengthened sheet can be made equal to the thickness of the plain cold-reduced sheet, or it can be somewhat reduced by the design-strengthening process; thus the weight per unit of projected area remains the same as that of a plain sheet or is reduced, thereby eliminating disadvantage (2). The workability of design-strengthened sheets is not limited as in the case of corrugated sheets, since the former can be stamped, drawn, formed, roll formed, spot welded or seam welded, thereby eliminating disadvantage (3). If advantageous, depending on the application, design-strengthened sheets can be subjected to a degree of cold working in order to further improve certain strength characteristics, or they can be subjected to a negligible amount of cold working so as to not affect their workability or ductility.

It is obvious that the degree of design-strengthening may be regulated within certain limits (a) by the design of the pattern itself and (b) by its depth.

Figs. 1a, 1b, and 1c show samples of design-strengthened surfaces. The particular patterns in Fig. 1a are referred to as No. 1 WL, No. 2 WL and No. 5 WL. (WL designates wavy line pattern.) Three degrees of depth are shown, No. 1 WL being the minimum and No. 5 WL the maximum for this type of pattern. It is important to observe the decrease in weight below that of the flat sheet and the increase in overall thickness. This decrease in weight per unit of area and increase in overall thickness serve to increase the effective *EI* (the stiffness factor) of the sheet per unit of weight.

Fig. 2 shows an enlarged transverse cross section where the maximum overall thickness occurs in a No. 5 WL pattern. In this figure is illustrated the brief definition of design-strengthening—*the redistribution of metal in flat sheets for the purpose of obtaining maximum strength-weight ratios and maximum rigidity-weight ratios.*

An important point is that the *end use* determines the geometric shape and dimensions of the pattern. In other words, the design engineer can devise or select the optimum finish for each and every application of design-strengthened materials. Displacement of metal can be increased to gain maximum rigidity (resistance to bending), or it can be decreased to meet other requirements of the finished parts. The radiuses of the lobes in the pattern may be increased to improve transverse-bending fatigue-stress values, or they may be reduced to secure maximum flexural rigidity if the latter value is of greater importance in the part being designed. *Plain areas* can be incorporated in the pattern for riveting or seam welding or for other purposes.

TENSILE PROPERTIES

Table 1 shows the tensile properties of plain and design-strengthened flat sheets of stainless steel (17–7). Table 2 shows the tensile properties of plain and design-strengthened flat sheet of carbon steel (SAE 1010) and

Presented at the Materials Session, Eleventh Annual Meeting, I.Ae.S., New York, January 25–29, 1943.

* President.

† Consultant, College of Engineering.

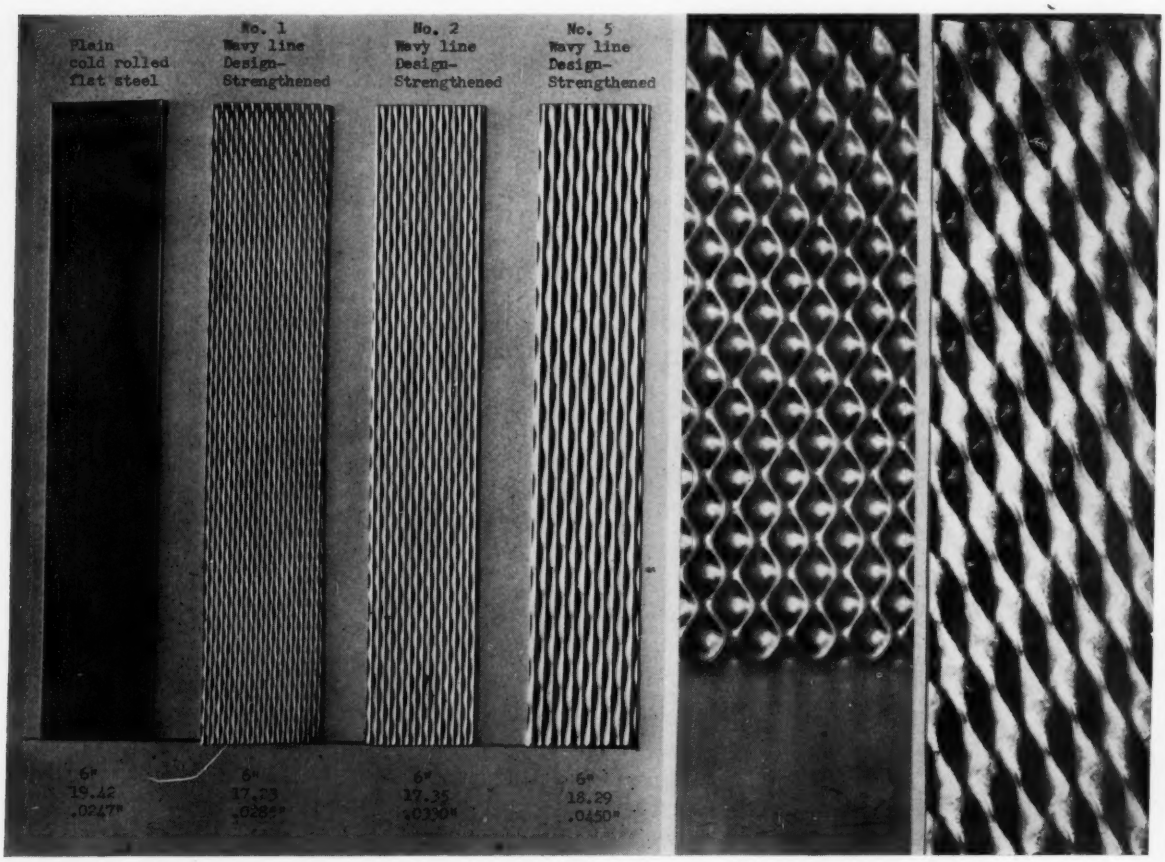

FIGS. 1a, 1b, and 1c. The length, weight in grams, and overall thickness of the specimens in Fig. 1a (*left*) are indicated under each piece. FIG. 1b (*middle*). Concave side of No. 6 WL Finish. Effective thickness increased 350 per cent or from 0.010 to 0.045 in. (Note parallel raised wavy lines forming opposing waves, all lines separated by sloped beads that are staggered and depressed.) FIG. 1c (*right*). Rigid-Tex special application design No. 1 ACC Finish (alternating concave and convex).

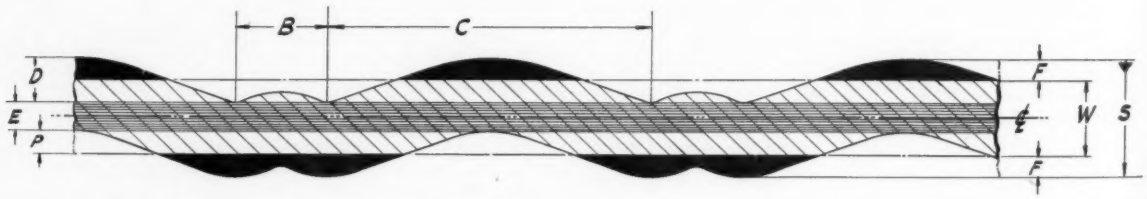

FIG. 2. Sample of enlarged transverse cross section approximately 18× of 24-gauge (0.025 in.) design-strengthened flat sheet. Wavy line pattern No. 5. Note *E* area of uniform cross section not found in regular corrugated sheet. Dark areas represent metal redistributed away from the neutral axis and beyond limit of plain cold-reduced sheet or strip.

A. $^1/_2$ in. Distance between successive crests of waves (see surface plan).
B. $^1/_{32}$ in. Distance between adjacent wavy lines at their closest point of approach.
C. $^7/_{64}$ in. Distance between adjacent wavy lines at their farthest distance apart.
D. 0.0145 in. Depth of finish from top of crest to bottom of line.
E. 0.0096 in. Area of uniform cross section.
F. 0.0145 in. Total maximum thickness of metal redistributed beyond limit of plain sheet.
P. 0.0154 in. Total maximum thickness of metal not redistributed and outside of *E*.
W. 0.0250 in. Original or weight thickness.
S. 0.0390 in. Effective or overall thickness.

chrome-molybdenum steel (X4130) steel. Table 3 shows the tensile properties of plain and design-strengthened flat sheet of aluminum alloy (Alclad 24).

Increases in proportional limits in design-strengthened (17–7) full-hard stainless steel (up 30 per cent in this case) result from uniformity of stress throughout the cross-sectional area, bearing in mind that plain cold rolling affects only the top and bottom surfaces, while design-strengthening affects both the surfaces and the cross-sectional areas and thus provides greater stress uniformity.

Fig. 3 shows typical tensile test specimens.

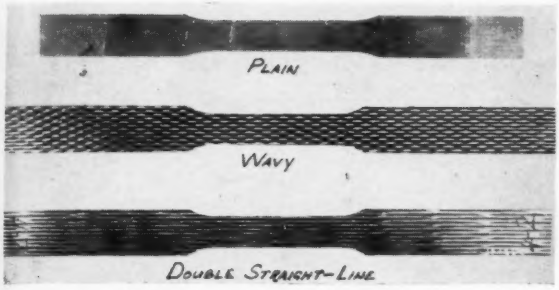

FIG. 3. Rigid-Tex tension specimens. Direction of rolling ←→.

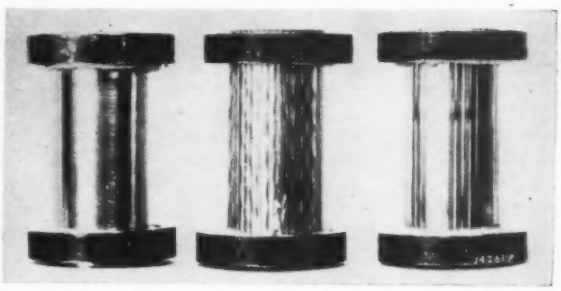

FIG. 4. Rigid-Tex compression cylinders after test.

TABLE 1

Tensile Properties of Design-Strengthened and Flat Sheets of Stainless Steel (17–7)

	Temper	Pln. C.R. Fin. Lbs. per Sq.In.	No. 2 WL D.-S. Fin. Lbs. per Sq.In.
Proportional limit (0.1 per cent offset)	1/4 hard	39,000	55,000
	Full-hard	46,000	59,000
Yield strength (0.2 per cent set)	1/4 hard	85,000	117,800
	Full-hard	162,000	154,000
Ultimate strength	1/4 hard	137,000	157,100
	Full-hard	179,000	194,000
Per cent elongation in 2-in. gauge length	1/4 hard	23	20
	Full-hard	10	10

NOTE: 40 per cent increase in overall thickness and 9 per cent decrease in minimum thickness.

TABLE 2

Tensile Properties of Design-Strengthened and Flat Sheets of Carbon Steel (SAE 1010) and Chrome-Molybdenum (X4130)

	SAE	Pln. C.R. Fin. Lbs. per Sq.In.	No. 2 WL D. S. Fin. Lbs. per Sq.In.
Yield strength (0.2 per cent set)	1010	22,200	57,000
	X4130	67,450	93,350
Ultimate strength	1010	46,950	60,900
	X4130	84,800	99,350

NOTE: 22 per cent increase in overall thickness and 35 to 11 per cent (4130) decrease in minimum thickness.

TABLE 3

Tensile Properties of Design-Strengthened and Flat Sheets of Aluminum Alloy (Alclad 24)

	Temper	Pln. C.R. Fin. Lbs. per Sq.In.	No. 5 WL D.-S. Fin.* Lbs. per Sq.In.
Yield strength (0.2 per cent set)	S-O	26,450	36,875
	S-T	37,750	38,650
Ultimate strength	S-O	37,100	43,150
	S-T	66,175	76,075

* Thickness S-O sheet—maximum up 100 per cent, minimum down 31 per cent; thickness S-T sheet—maximum up 45 per cent, minimum down 33 per cent. Micro-examination (at 500×) show Alclad layer intact and unaffected by Rigid-Tex Process with regard to quality.

TABLE 4

Buckling Stress of Design-Strengthened and Flat Sheets of Stainless Steel (17–7 Full-Hard)

	Pln. C.R. Fin. Lbs. per Sq.In.	No. 2 WL D.-S. Fin.* Lbs. per Sq.In.
Buckling strength	168,000	172,000
Yield strength (0.2 per cent offset)	111,000	139,000
Proportional limit (0.01 per cent offset)	44,000	59,800
Modulus of elasticity	28,000,000	27,200,000

* Overall thickness increased 34 per cent; minimum thickness reduced 17 per cent; yield strength increased 26 per cent: proportional limit increased 35 per cent.

BUCKLING STRENGTH

The buckling stress was determined by the cylinder test method (see Fig. 4). This method consists, briefly, of determining the compressive stress-strain characteristics of a cylindric sample having a slenderness ratio of 5 and a diameter to wall thickness ratio of 40. The cylinders were tested in compression in a 200,000-lb. capacity Baldwin-Southwark hydraulic testing machine. The deformation was measured with a pair of Tuckerman optical strain gauges located diametrically opposite each other. The tests were made in a special compression jig consisting of a hardened steel plunger and spherical seat in a cast-iron holder to minimize any effects of unequal loading or movement of the testing machine heads.

The compressive characteristics of plain and design-strengthened sheet stainless steel (17–7), full-hard, are shown in Table 4. Similar improvements are noted in Table 5 for carbon and chrome-molybdenum steels.

FLEXURAL RIGIDITY

The flexural rigidity of design-strengthened flat sheet depends, as already mentioned, (a) upon the particular design used and (b) upon the depth of the impression or the effective overall thickness of the sheet. For ex-

TABLE 5

Buckling Stress of Design-Strengthened and Flat Sheets—Carbon (SAE 1010) Steel and Chrome-Molybdenum (X4130) Steel

Finish	SAE 1010 Carbon Buckling Strength, Lbs. per Sq.In.	Per Cent Increase		SAE X4130 Chrome-Molybdenum Buckling Strength, Lbs. per Sq.In.	Per Cent Increase		Remarks
		Buckling strength	Overall thickness		Buckling strength	Overall thickness	
Plain cold-rolled	32,700			61,300			Tests transverse to the pattern show an increase of 15 per cent over plain C.R. transverse
Design-strengthened No. 2 WL fin.	55,250	70	22	88,500	44	30	

TABLE 6

Improvement of Flexural Rigidity (*EI*) of Flat Sheet Stainless Steel (17-7 Full-Hard) by Design-Strengthening—No. 5 Wavy Line Pattern

Finish	Specimen, Weight, Gm.	*EI*, In. and Lb. Units	Per Cent Increase		Remarks
			EI	Overall thickness	
Plain cold-rolled	11.770	14.29			Thickness 0.0182 in.
Design-strengthened	11.770	25.88	81	95	

TABLE 7

Improvement of Flexural Rigidity (*EI*) of Flat Sheet Carbon Steel (SAE 1010) by Design-Strengthening—No. 2 Wavy Line Pattern

Finish	Specimen, Weight, Gm.		*EI*, In. and Lb. Units	Per Cent Increase		Remarks
				EI	Overall thickness	
Plain cold-rolled	Transverse	17.576	47.6			Thickness 0.0310 in.
	Longitudinal	18.655	59.0			
Design-strengthened	Transverse	17.576	56.9	19.5	22	
	Longitudinal	18.655	67.4	14.2		

TABLE 8

Improvement of Flexural Rigidity (*EI*) of Flat Sheet of Aluminum Alloy (24)*, by Design-Strengthening—No. 5 Wavy Line Pattern

Finish	Heat-Treatment	Weight Gm.	*EI*, In. and Lb. Units	Per Cent Increase		Remarks
				EI	Effective thickness	
Plain cold-rolled	S-O	4.601	7.24			Thickness 0.0207 in.
	S-T	4.596	7.16			
Design-strengthened	S-O	4.601	15.07	108	100	
	S-T	4.596	13.90	94	92	

* It has been established that the effect of the Rigid-Tex process in increasing flexural stability is practically entirely due to the design or pattern. This conclusion is drawn from the fact that the percentage increase in yield strength in bending for heat-treated 24 S-O, which increase was to design only, was as high as the percentage increase in the 24 S-T of the same design or pattern.

ample, it is to be expected, with reference to Fig. 1a, that No. 5 WL specimen will show more improvement in rigidity than No. 1 WL.

Tables 6, 7, and 8 show sample tests selected at random and are for comparative purposes only. The *EI* values in these tables were obtained (see Fig. 5) by loading the specimen (about $^5/_8$ in. wide and 5 in. long), supported at the ends, by a concentrated load, P, at the center; and by noting the deflection, y, at the center. If L is the length of the specimen between supports, *EI* is computed from the formula:

$$EI = PL^3/48y \qquad (1)$$

IMPACT DEFORMATION

Description of Test: A 1-in. diameter steel ball mounted on the end of a tube $^5/_8$-in. diameter and 12 in. long was used as a falling plummet. The tube was filled with lead for approximately one-third of its length from the ball in order to increase the weight and move the center of gravity toward the ball. Fins were attached to the upper end of the tube to direct its travel. Discs, 4 in. in diameter, were prepared from No. 4 commercial finishes and the Rigid-Tex design-strengthened finishes, and these were held between two wooden rings of 4-in. outside diameter with a bore 2 in. in diameter. Thus a 2-in. diameter area at the center of

TABLE 9

Impact Deformation of Design-Strengthened and Flat Sheets of Stainless Steel (18–8 Cold-Rolled, Annealed, and Polished)

Gauge No.	Height of Fall of 1.02-Lb. Plummet	Inches Depth of Deformation				
		No. 4 finish	D.-S.* No. 1 WL	Per cent less def.	D.-S.* No. 2 WL	Per cent less def.
28	11 ft. 7 1/2 in.	0.247	0.207	20	0.221	11
26	11 ft. 7 1/2 in.	0.232	0.179	29	0.221	10
24	11 ft. 7 1/2 in.	0.218	0.165	32	0.171	31
22	11 ft. 7 1/2 in.	0.187	0.148	26	0.148	30
20	11 ft. 7 1/2 in.	0.191	0.177	8	0.127	50
18	11 ft. 7 1/2 in.	0.118	.....	...	0.072	64

* D.-S. = design-strengthened and WL = wavy line specimen.

NOTE: Average percentage increase in effective or overall thickness for No. 1 WL pattern from 20 to 22 gauge was 17 per cent, while the average percentage increase for the No. 2 WL pattern was 32 per cent. It will be noted that the latter pattern increase is about twice the former; this conforms with the original geometric plan, since No. 2 WL was designed to be about twice the size and depth of No. 1 WL pattern.

the discs was unsupported. The rings were compressed by means of a hollow cylinder weighing 365 lbs. The plummet was suspended directly over the center of the test disc by means of a cotton string and was released by burning the string. Comparative resistance to impact deformation for the two types of finishes was determined by measuring the depth of impression with a depth micrometer. Table 9 shows test results on several samples.

CONCLUSIONS

Tensile, buckling, flexural rigidity and impact deformation tests were made on specimens from 17–7 stainless, chrome-molybdenum (X4130), and carbon (1010) steels, and also on aluminum alloys. The results of these tests warrant the following conclusions:

(1) For full-hard stainless steel, design-strengthening has no significant effect on the tensile properties, except on the proportional limit which shows a substantial increase. For chrome-molybdenum and carbon steels an increase in yield and ultimate strengths was indicated; this also applies to the aluminum alloys.

(2) For full-hard stainless steel, design-strengthening produces important increases in proportional limits and yield strengths of cylindric specimens in compression longitudinally and transversely. The same applies to chrome-molybdenum and carbon steels.

(3) For full-hard stainless, chrome-molybdenum, and carbon steels design-strengthening produces important increases in flexural rigidity (*EI*). This also applies to aluminum alloys. Greater relative increase in rigidity is noted with (a) thinner sheets, (b) softer sheets, and (c) sheets having greater increase in overall or effective thickness.

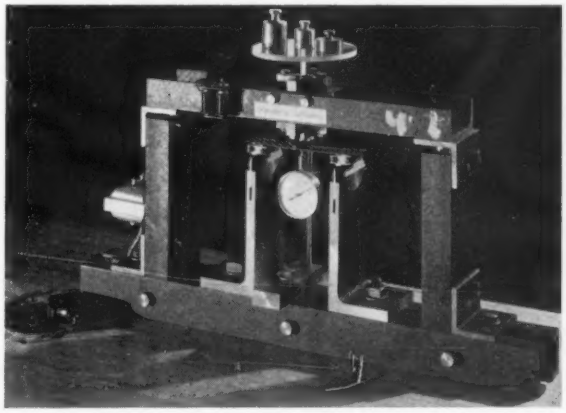

FIG. 5. Rigid-Tex apparatus used to determine the *EI* of design-strengthened versus plain materials by the simple beam test.

(4) For cold-rolled and annealed stainless steel, design-strengthening produces greater resistance to impact deformation.

(5) For stainless steel and for Alclad 24 S-T design-strengthening shows no effect in the salt spray test. Alclad 24 S-T, whether design-strengthened or plain, showed only a superficial surface attack, natural for Alclad material under this test. The specimens were subjected to a 20 per cent sodium-chloride spray for 284 hours and were then microscopically examined. Stainless-steel samples showed no appreciable corrosion after 100 hours' salt spray at room temperatures.

Buckling of Aluminum-Alloy Columns and Plates

HENRY L. LANGHAAR*

Consolidated Vultee Aircraft Corporation

SUMMARY

By means of an argument based on the effective modulus theory, a method has been devised for simultaneously plotting buckling curves for columns and for plates. The usefulness of the method lies in the fact that, with column data only, it permits the estimation of compression buckling stresses for plates with various edge conditions, when these stresses exceed the compression proportional elastic limit of the material. Some composite plate and column curves for 24S aluminum alloy are presented, and a method for applying them to the design of hat-type plate-stringer combinations is proposed.

TEST SPECIMENS

THE FOLLOWING THREE SETS of columns were tested:

Set 1—$^7/_8$ in. diameter solid rolled rods. These are subdivided into the following groups: (A) 24S-T as-received; (B) 24-RT (stocked 24S-T rod heated 920° for 34 min. and quenched in water. Then stretched to $3^1/_2$ per cent set and aged 96 hours at room temperature).

Set 2—No. 30159 extrusions (Fig. 1). These are subdivided into the following groups: (A) 24S-T as-received; (B) 24-RT (same treatment as Set 1(B)).

Set 3—$^1/_4$ by $1^1/_2$ in. strips of aluminum-alloy sheet. All strips ran with the sheet grain. Set 3 is subdivided into the following groups: (A) 24S-T as-received; (*B*) 24-RT (same treatment as Set 1(B)); (C) 24S-T Alclad as-received; (D) 24-RT Alclad (same treatment as Set 1(B)).

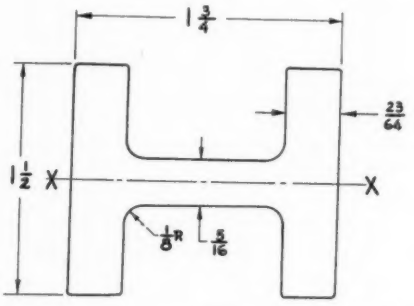

FIG. 1. Area = 1.414; $\rho = 0.381$. Knife edge on axis X–X.

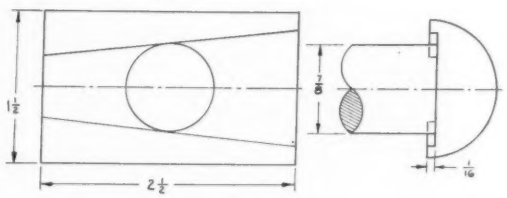

FIG. 2.

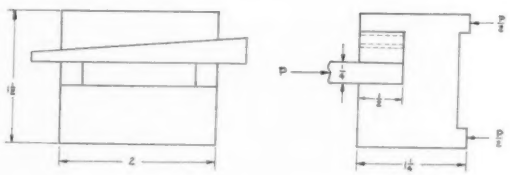

FIG. 3.

PROCEDURE

The columns of Sets 1 and 2 were tested with case-hardened semicylindric steel roller heads, $1^1/_2$ in. diameter by $2^1/_2$ in. length. The rollers had tapered slots $^1/_{16}$ in. deep for centering the rods of Set 1 (Fig. 2). For the purpose of testing the extruded columns, 24S-T strips were inserted in the slots to render flush bearing surfaces.

For testing the strip columns, slotted chrome-molybdenum steel blocks and wedges were used to grip the ends of the specimens (Fig. 3). As shown in Fig. 3, the edges of the blocks were lipped to give reactions as in a simple beam. The load naturally tended to close the slots and to cause a grip pressure approximately equal to the bending stress that would have existed in unslotted blocks.

The ends of all columns were ground flat and parallel, and care was taken to seat them properly in their retainers. The specimens were tested in a 400,000-lb. Southwark-Emery machine. Flat, case-hardened, steel bearing blocks were used to transmit the loads to the heads on the columns. The specimens were set up vertically with the aid of a level and, in the case of the roller-ended columns, the roller heads were lined up against a flat board to ensure parallelism.

By means of a stress-strain recorder, compression stress-strain curves were taken from two samples of each group of columns.

Presented at the Structures Session, Eleventh Annual Meeting, I.A.S., New York, January 25–29, 1943.

* Structural Research Engineer.

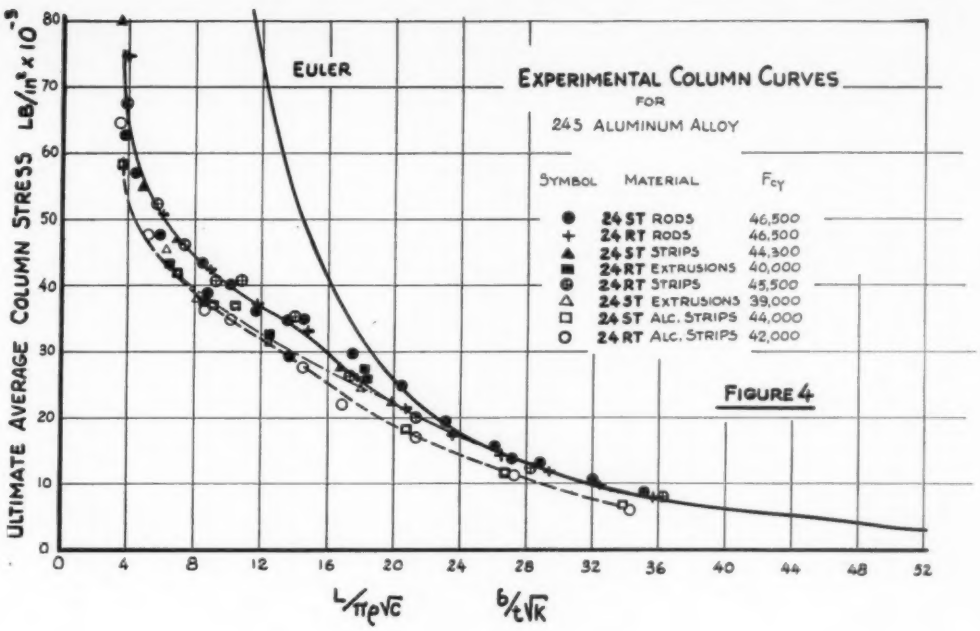

FIGURE 4

End Fixity in the Tests

The effective length of a roller-headed column is the distance between roller centers.* Ideally, there is no end fixity (i. e., $C = 1$), since the load, passing through the center of the roller, gives zero moment on the end of the column. The fixity factor for a column with rigidly clamped ends is $C = 4$.

It was found that the ideal fixity factor was practically realized by the roller-ended columns but that the value $C = 3.6$ for the clamped-ended columns provided a smooth junction with the Euler curve. To insure the constancy of the fixity factors, a few highly heat-treated chrome-molybdenum steel columns were tested. Because of their higher moduli and higher yield stresses, these columns carried much higher loads in the Euler range than the aluminum-alloy columns. However, no deviation from the respective fixity factors $C = 1$ and $C = 3.6$ was perceived in the range of stresses where the Euler formula could be applied, and it is concluded that these factors apply for all of the columns.

Results

Column test points and compression yield stresses for the various groups of columns are recorded in Fig. 4. For reasons that will be explained, the abscissa on these curves is $L/\pi\rho\sqrt{C}$; i.e., ultimate average stresses for columns of Sets 1 and 2 were plotted against $L/\pi\rho$, and ultimate average stresses for columns of Set 3 were plotted against $L/\pi\rho\sqrt{3.6}$.

* Accordingly, the effective lengths of the extruded columns were $^1/_8$ in. greater than their measured lengths.

Column Charts

Euler's formula for a column with end fixity C may be expressed

$$L/\pi\rho\sqrt{C} = \sqrt{E_e/\sigma_{cr}} \qquad (1)$$

in which E_e, the effective modulus, is a function of the average† stress σ. Thus, one curve of σ_{cr} vs. $L/\pi\rho\sqrt{C}$ will cover all conditions of end fixity.

Except for a slight lack of conformity shown by the 24S-T rolled rods,‡ the column curves of the present tests (Fig. 4) are in good agreement; i.e., columns with equal compression yield stresses fall on a common curve. It is noted that no significant form effect is manifested by the differences in the column cross sections.

The agreement between curves for columns with the same compression yield stress suggests the construction of a family of column curves for 24S aluminum alloy with compression yield stress as a parameter. This can be effected by interpolating between the curves of Fig. 4. Fig. 5 is the resulting column chart.** The

† Simple theoretic considerations lead to the conclusion $E_e = E_t$, the slope of the stress-strain curve. However, in practice deviations from this relation are observed (see heading "Effective Modulus vs. Tangent Modulus" of this report).

‡ The slightly different character of the column curve for 24S-T rolled rods can probably be attributed to lighter mechanical treatment in rolling. Grain characteristics are known to exert a strong influence on plastic properties of metals (The Engineering Societies monograph "Theory of Plasticity" by Nadai).

** The Alclad columns have been disregarded in the construction of this chart. Because of insufficient data, an Alclad column chart has not been constructed, but the dotted curve of Fig. 4 may be used for Alclad with a compression yield stress between 42,000 and 44,000 lbs. per sq.in.

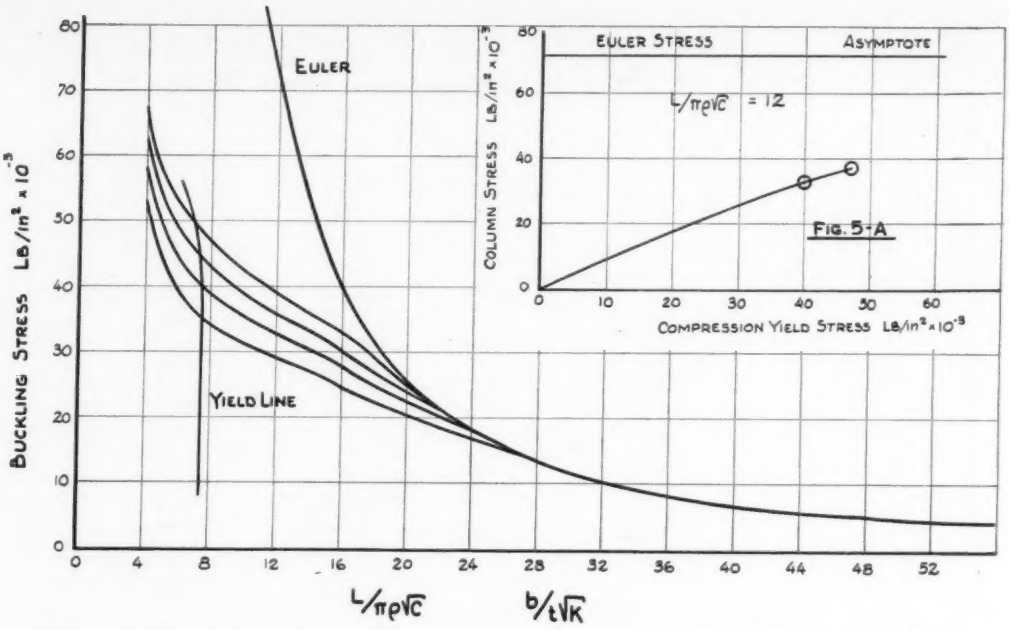

FIG. 5. Buckling chart 24S aluminum-alloy sheets and extrusions. FIG. 5-A. Sample interpolation curve.

compression yield stress correspondng to a given curve on this chart is indicated by the ordinate of its intersection with the yield line. This is an adaptation of the familiar device used for denoting the yield stress on a stress-strain curve.

As an example of the method of interpolation used in the construction of the chart, the points in Fig. 5 corresponding to $L/\pi\rho\sqrt{C} = 12$ are computed. The test data (Fig. 4) supply the four stresses at $L/\pi\rho\sqrt{C} = 12$, shown in Table 1.

These four points provide a curve (Fig. 5-A), from which the values in Table 2 are picked.

These values are plotted on Fig. 5 at $L/\pi\rho\sqrt{C} = 12$. The same procedure provides points on the lines $L/\pi\rho\sqrt{C} = 4, 6, 8, 10$, etc.

BUCKLING OF PLATES

The buckling stress for a flat plate under compression or shear is given by

$$b/t\sqrt{K} = \sqrt{E_e/\sigma_{cr}} \qquad (2)$$

where b is the width, t is the thickness, and K is a factor depending on the aspect ratio, the edge fixities, and the type of loading.* The Poisson-ratio factor, which usually appears in formulas for buckling of plates, is here incorporated with K. It is a fundamental assumption of the present theory that the effective moduli E_e for columns and for plates are identical. It is then evident from a comparison of Eqs. (1) and (2) that identical functions of the respective arguments $L/\pi\rho\sqrt{C}$ and $b/t\sqrt{K}$ define the buckling stresses for columns and for plates. Thus, the buckling stress for a plate is obtained simply by interpreting the abscissa of the buckling chart to be $b/t\sqrt{K}$ rather than $L/\pi\rho\sqrt{C}$.

TABLE 1

F_{cy}	0	40,000	46,500	∞ (Euler)
σ_{cr}	0	32,500	36,700	71,500

TABLE 2

F_{cy}	35,000	40,000	45,000	50,000
σ_{cr}	29,000	32,500	35,800	38,500

BUCKLING OF FORMED ALCLAD COLUMNS

It may be assumed that the aluminum coat does not appreciably influence the core buckling stress of a rolled or drawn Alclad column or stringer of sufficiently heavy cross section to preclude local failures.

It is then possible to construct curves for formed Alclad columns, but they differ by less than 2 per cent from the curves of Fig. 5. Accordingly, the construction of Alclad column curves is an insignificant refinement, and the curves of Fig. 5 may be used without modification for formed Alclad columns. It should not be inferred that Fig. 5 applies for the buckling of Alclad plates, however. For this case, reference should be made to Fig. 4.

EFFECTIVE MODULUS VS. TANGENT MODULUS

It is interesting to ascertain how well the tangent modulus E_t approximates the effective modulus E_e

* *See* A.C.T.R. 4313 Rev. No. 1, Fig. 2-2 for values of K with compression loading and simple edge conditions.

in the present tests. To this end it is noted that, since $E_t = d\sigma/d\epsilon$, the strain ϵ is given by

$$\epsilon = \int_0^\sigma d\sigma/E_t \tag{3}$$

Substituting E_e for E_t and performing the integration numerically, one may compute a modified stress-strain curve whose slope, corresponding to the stress σ, is E_e.

By means of the data of Fig. 4, a curve of this type (Fig. 6) has been constructed for the 24-RT rolled rods, the effective moduli E_e being determined by Eq. (1).

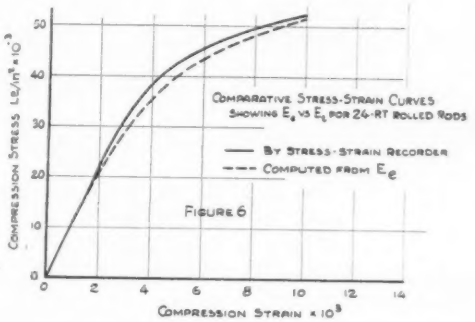

The stress-strain curve by a strain recorder is also shown on Fig. 6. It is seen that at points with the same ordinate the slope of the effective stress-strain curve is less than the slope of the true stress-strain curve; i.e., in general, $E_e < E_t$.

The Straight-Line Approximation

It is evident from an inspection of Fig. 5 that the buckling stress for 24S aluminum alloy can be closely approximated by a straight line in the interval between the Euler curve and the yield line. Denoting the intercept of this line with the stress axis by F_{c0} (Fig. 7), we obtain from Fig. 5 the relation

$$F_{c0} = 1.20F_{cy} \tag{4}$$

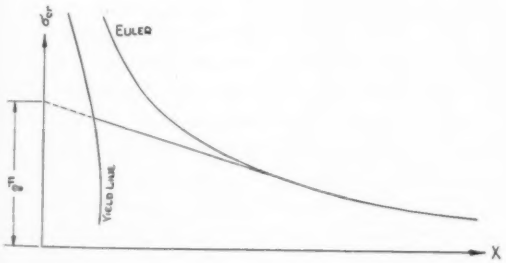

FIG. 7.

Thus, an approximate buckling curve for 24S aluminum alloy with known compression yield stress is easily constructed.

Letting X denote $L/\pi\rho\sqrt{C}$ or $b/t\sqrt{K}$ (when column buckling or plate buckling, respectively, is under consideration), the equation of the Euler curve is obtained in the form

$$\sigma_{cr} = E/X^2 \tag{5}$$

The equation of the tangent line is

$$\sigma_{cr} = F_{c0}\,[1 - {}^2/_3\sqrt{F_{c0}/3E}\;X] = F_{cy}\,[1.2 - 0.506\sqrt{(F_{cy}/E)}\;X] \tag{6}$$

Eqs. (5) and (6) are approximate analytic expressions for the buckling chart Fig. 5. Eq. (5) will apply in the range $X > 1.58\sqrt{E/F_{cy}}$, and Eq. (6) in the range $X < 1.58\sqrt{E/F_{cy}}$, $\sigma_{cr} < F_{cy}$.

Hat-Type Stringer-Plate Combinations

A typical cross section of a hat-type stringer-plate combination is shown in Fig. 8. In addition to the notations shown in Fig. 8, the following notations are used:

- L = length of the plate-stringer combination (in a wing, this is the bulkhead spacing)
- ρ = radius of gyration of the entire plate-stringer combination cross section
- A_s = cross-sectional area of a stringer
- p = rivet pitch
- d = rivet diameter
- P = ultimate load per panel
- σ_{sf} = stringer stress to cause local failure
- σ_{sc} = stringer stress to cause column failure
- σ_s = ultimate stringer stress—i.e., the smaller of the two values σ_{sc} and σ_{sf}
- σ_{ps} = stress in the plate corresponding to the stringer stress σ_s (if the plate and the stringers are of the same material, then $\sigma_s = \sigma_{ps}$)
- σ_{pr} = stress in the plate to cause buckling between the rivets
- σ_m = maximum stress in the plate—i.e., the smaller of the values σ_{ps} and σ_{pr}
- σ_{cr1}, σ_{cr2} = buckling stresses for the respective spans b_1 and b_2
- W_1, W_2 = effective widths of plate corresponding to the spans b_1 and b_2 (Fig. 8)

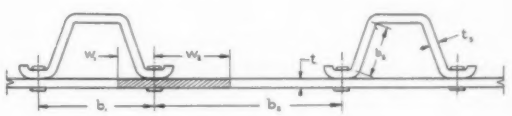

FIG. 8.

The load P is determined by the relation

$$P = \sigma_s A_s + 2t(W_1 + W_2)\sigma_m \tag{7}$$

The problem thus resolves itself into the determination of the stresses σ_s, σ_m, and the effective widths W_1, W_2.

The Stress σ_s

The stress σ_{sf} corresponds to the abscissa $b_s/t_s\sqrt{K}$ on the buckling chart (Fig. 4 or 5). When the flat section of side wall is terminated by fillets, it is found that the dimension b_s is effectively greater than the width of the flat portion. In these cases, the measurement of b_s between the centroids of the bend areas has been found to give good results, even with fillet radii as great as $^3/_4$ in. The dimension b_s should be measured across the top of the hat section if the width of the top is greater than the width of the side wall.

The fixity factor K is difficult to determine accurately, since only $\sqrt{K}$ is used in computations. A study of data from several hundred plate-stringer test specimens indicates that $\sqrt{K} = 2.3$ is the best average value.

The stress σ_{sc} corresponds to the abscissa $L/\pi\rho\sqrt{C}$ on the buckling chart (Fig. 5). In the design of a wing, the fixity factor C is specified. For the interpretation of flat-ended plate-stringer tests, it is found best to regard C as a linear function of L/ρ, which increases from $C = 3$ at $L/\rho = 0$ to $C = 3.6$ at $L/\rho = 80$, and thereafter remains constant. No doubt, as L/ρ becomes large, C must decrease to the limit unity, because of the effect of irregularities such as initial curvature, eccentric loading, inhomogeneous materials, etc. However, the range of decreasing C is not reached with practical lengths of plate-stringer test specimens.

The allowable stringer stress σ_s is the smaller of the two values σ_{sc} and σ_{sf}.

The Stress σ_m

The stress σ_{ps} is determined by comparative stress-strain curves for the plate material and the stringer material (Fig. 9).

The stress σ_{pr} is conditioned by the rivet pitch. Buckling of the sheet between the rivets is essentially the failure of a column of length $(p - d)$ and radius of gyration $t/\sqrt{12}$. The fixity in this case has not yet been definitely established. Assuming $C = 4$, the abscissa on the buckling chart becomes $\sqrt{3}\,(p - d) \div \pi t$. σ_m is the smaller of the two values σ_{ps} and σ_{pr}.

The Effective Widths

It is assumed that the stress distribution between consecutive rivet rows is a simple cosine wave with the maximum value σ_m on the lines of rivets and the minimum value σ_{cr} midway between the lines of rivets.

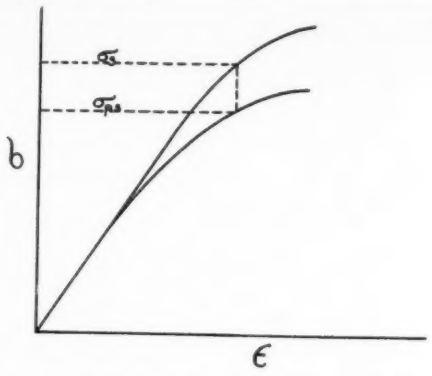

FIG. 9. Upper curve for stringer. Lower curve for plate.

This assumption leads to the von Kármán effective width formulas*

$$\left.\begin{aligned} W_1 &= {}^1/_4 b_1(1 + \sigma_{cr1}/\sigma_m) \\ W_2 &= {}^1/_4 b_2(1 + \sigma_{cr2}/\sigma_m) \end{aligned}\right\} \qquad (8)$$

for the two spans b_1 and b_2. The stresses σ_{cr1} and σ_{cr2} correspond to the abscissas $b_1/t\sqrt{K}$ and $b_2/t\sqrt{K}$ on the buckling chart. By noting the stresses at which plate buckling occurred in plate-stringer combinations, it has been ascertained that $\sqrt{K} = 2.2$ for this case.

The preceding method has been used to study the results of several hundred plate-stringer tests of the Consolidated Vultee Aircraft Corporation, and it has been found to be accurate within ± 10 per cent when the buckling stress of the plate is greater than 15 per cent of the allowable stringer stress σ_s. However, when the buckling stress of the plate is less than this amount, the method becomes unconservative because of limitations of the effective-width formula.

CONCLUSIONS

(1) The dotted curve in Fig. 4, corresponding to the abscissa $b/t\sqrt{K}$ determines buckling stresses for 24S Alclad sheets with compression yield stresses in the range 42,000 to 44,000 lbs. per sq. in.

(2) The curves of Fig. 5 determine buckling stresses for 24S columns and sheets, and for 24S Alclad columns.

(3) The charts may be used for the analysis of hat-type plate-stringer combinations, as described under the heading "Hat-Type Stringer-Plate Combinations."

* *See* A.C.T.R. 4313 Rev. No. 1, Eq. 4-14.

Regions of Infinite Acceleration and Flow Realms in a Compressible Fluid

MAX G. SCHERBERG*
United Aircraft Corporation

SUMMARY

When a body moves in a compressible fluid at speeds comparable to the speed of sound in the fluid, then there will exist, in general, regions of fluid near the body in which the speed relative to the body is supersonic. Experience in the wind tunnel and in flight has shown that such flows are usually accompanied by shock waves, as a result of which there is, among other things, a large increase of drag coefficient. Since shock waves are being associated with the presence of flow conditions,[1] which call for regions of infinite acceleration, it becomes important to determine the circumstances under which such regions are present and to seek methods of avoiding these conditions.

A PRELIMINARY INVESTIGATION of the Navier-Stokes equations for viscous flow has indicated that in the case of a simple radial airflow the viscosity effects are negligible until the accelerations become large. Investigations by Taylor[2] and others indicate that flow in the shock wave is not adiabatic and that the viscous forces are important. The inference seems to be that the shock wave flow puts in an appearance in order to make possible a flow that would otherwise require infinite acceleration—just as Kutta explained the presence of circulation to make possible flow over a lifting airfoil without encountering infinite accelerations at the trailing edge. In the former the large accelerations appear because of the physical properties of the compressible fluid, whereas in the latter it is a matter of flow around a corner.

In a recent paper,[1] some conditions were specified under which regions of infinite acceleration may be located and also the conditions that should be satisfied in a flow if such regions are to be absent. A more complete set of such conditions is developed here, and it is shown that in a compressible fluid, flowing under the isentropic relation $p = k\rho^{\gamma}$, there may exist, in general, two realms of flow, which have been labeled as minus $(-)$ and plus $(+)$ realms. The minus realm may consist of both subsonic and supersonic flow, but the flow conditions are like those of ordinary subsonic flow. The plus realm is entirely supersonic, and its flow conditions are distinct from those in the ordinary subsonic flow.

SIMPLE FLOWS

The paper will be developed by first examining three well-known simple flows, which will illustrate some of the points mentioned and will also aid in developing the general result.

Assume a two-dimensional steady flow in a plane in which the symbols r, θ, v, ω, α, P and ρ represent, respectively, the following quantities: r, θ are the polar coordinates of a fluid particle position in the flow; v, the radial component of the velocity; ω, the angular velocity; α, the angular acceleration; P, the pressure at the position (r, θ); and ρ, the density at (r, θ). There is need for the following equations:

$$\dot{v} - r\omega^2 = -(1/\rho)(\partial P/\partial r) \tag{1}$$

$$2v\omega + r\alpha = -(1/\rho)(\partial P/r\partial\theta) \tag{2}$$

are the equations of motion in which the left-hand members are the radial and transverse components of the acceleration of a particle and $\dot{v}$ is the time derivative of v as the particle moves along its stream line. The equation of continuity is

$$(\partial(\rho v r)/\partial r) + (\partial(\rho r\omega)/\partial\theta) = 0 \tag{3}$$

and

$$2\omega + r(\partial\omega/\partial r) - [(1/r)(\partial v/\partial\theta) = 0 \tag{4}$$

is the equation for zero rotation. On expanding Eq. (3) and making use of the notation

$$dP/d\rho = a^2 \tag{5}$$

in which a is usually described as the local speed of sound, it is found, with the help of Eqs. (1) and (2), that

$$\frac{rv}{a^2}(\dot{v} - r\omega^2) - \frac{\partial v}{\partial r}r - v + \frac{r^2\omega}{a^2}(r\alpha + 2\omega v) - r\frac{\partial\omega}{\partial\theta} = 0 \tag{6}$$

RADIAL FLOWS

Assume a radial flow whose stream lines coincide with the lines θ = const. and are such that v and $\dot{v}$ are independent of θ. Thus ω and α are both identically zero and Eq. (6) reduces to

$$\{[(v\dot{v}/a^2) - (\partial v/\partial r)]r\} - v = 0 \tag{7}$$

Since v is independent of θ,

$$\partial v/\partial r = dv/dr = \dot{v}/v$$

and Eq. (7) may then be solved for the acceleration in the form

$$A = \dot{v} = [a^2 v^2/r(v^2 - a^2)] \tag{8}$$

Received October 21, 1942.

* Mathematician in Aerodynamics, Chance Vought Aircraft Division.

Four variations of this type of flow are shown in Fig. 1. Note first that the flow must remain outside the circle on which $v^2 = a^2$ since the sign of A would preclude the possibility of a continuous flow from the inside up to the periphery of the circle. Further, note that there are two distinctive types of flow outside this circle. The first consists of the flows (1) and (2) (see Fig. 1), in which the acceleration (hence, the pressure gradient) has the direction in which the flow channel is closing. The second consists of the flows (3) and (4), in which the acceleration (hence, the pressure gradient) has the direction in which the flow channel is opening. Although these two fundamental types of flow are also distinguished by the fact that one is subsonic while the other is supersonic, it will be shown later that this feature is not always present. For reasons to be indicated later, these fundamental flows will be described as the minus and plus realms.

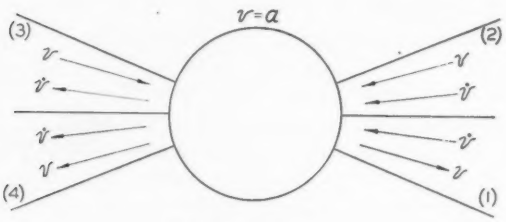

FIG. 1. Radial flows.

The region about $v^2 = a^2$ is a region of infinite acceleration, and this is true whether the channels are opening or closing or whether the flow is subsonic or supersonic. Finally, it can be readily verified that the flows are irrotational.

CIRCULAR FLOWS

Assume a circular flow whose stream lines coincide with the concentric circles r = const. and are such that ω and α are independent of θ. Thus v and $\dot{v}$ are both identically zero and Eq. (6) is automatically satisfied. By means of Eq. (4), for irrotational motion,

$$2\omega + r(\partial\omega/\partial r) = 0 \tag{9}$$

and, hence since $\partial\omega/\partial r = d\omega/dr$, Eq. (9) may be solved to give

$$\omega = c/r^2 \tag{10}$$

in which c is a constant of integration. Thus the acceleration in this case is

$$A = -r\omega^2 = -c^2/r^3 \tag{11}$$

This flow may be either counterclockwise or clockwise. It contains regions of both subsonic flow and supersonic flow, but the entire flow will be established as of the minus realm. The channel lines across a constant pressure fluid line, such as dc, are parallel in contradistinction to the converging and diverging lines of the preceding flows. In fact these lines are parallel to the constant pressure lines—that is, the flow is normal to the pressure gradient. Here also the flow must lie outside of some circle about the pole of the coordinate system, since in the ideal compressible fluid the maximum speed attainable in the fluid is well defined by the formula $V_m = \sqrt{[2/(1-\gamma)]}a_0^1$ in which a_0 is the velocity of sound in the fluid at rest and $\gamma = c_p/c_v$, the quotient of specific heat at constant pressure to that at constant volume. From Eqs. (10) and (11) it can be shown that this flow has a maximum acceleration $A_m = V_m^3/c$ and, hence, the flow is free of regions of infinite acceleration.

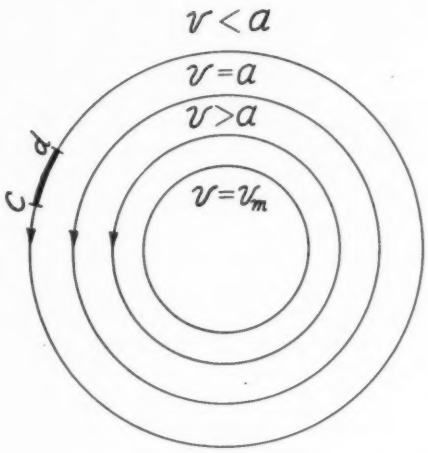

FIG. 2. Circular flow.

THE CORNER FLOW

In this case assume that v and $r\omega$ are not functions of r so that Eq. (6) becomes

$$\frac{vr}{a^2}(\dot{v} - r\omega^2) - v + \frac{r^2\omega}{a^2}(r\alpha + 2v\omega) - r\frac{\partial\omega}{\partial\theta} = 0 \tag{12}$$

Since $dv/d\theta = \partial v/\partial\theta$ and

$$\partial(r\omega)/\partial r = \omega + r(\partial\omega/\partial r) = 0 \tag{13}$$

Eq. (4), for zero rotation, becomes

$$2\omega + r(\partial\omega/\partial r) - (\dot{v}/r\omega) = 0 \tag{14}$$

on combining Eqs. (13) and (14),

$$\dot{v} - r\omega^2 = 0 \tag{15}$$

From Eq. (13) and

$$\alpha = (\partial\omega/\partial r)v + (\partial\omega/\partial\theta)\omega \tag{16}$$

the following equation is formed

$$\partial\omega/\partial\theta = (\alpha/\omega) + (v/r)$$

Eq. (6) may now be written

$$\{[(r\omega)^2/a^2] - 1\}(r\alpha + 2v\omega) = 0 \tag{17}$$

This flow may consist of two types such as shown in Fig. 3. If the second part of Eq. (17) is set equal to zero, then both components of the accelerations are zero and the flow is uniform, as in cases (1) and (3) in Fig. 3. The other alternative is that in which

$$(r\omega/a)^2 - 1 = 0 \tag{18}$$

and in that case there will be a curved flow such as case (2) in the Fig. 3. To determine the acceleration for the part $r\omega = a$ in Eq. (18)

$$(d/dt)(r\omega) = v\omega + r\alpha = da/dt \tag{19}$$

and, hence, the acceleration may be written

$$A = 2v\omega + r\alpha = (1/r)[d(ar)/dt] \tag{20}$$

To reduce this further

$$P = (P_0/\rho_0\gamma)\rho^\gamma \tag{21}$$

in which the zero subscript indicates rest conditions and γ is the ratio between the specific heats at constant pressure and constant volume.

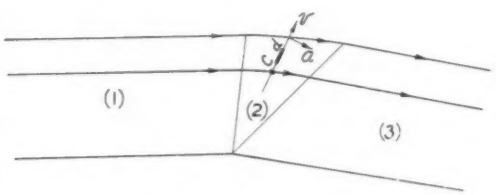

FIG. 3. Corner flow.

On combining Eqs. (1) and (2),

$$d(V^2/2) = -(1/\rho)dP \tag{22}$$

in which V is the speed of the fluid. From Eqs. (5) and (21)

$$d(a^2) = (\gamma - 1)(dP/\rho) \tag{23}$$

and, hence, from Eqs. (22) and (23)

$$a^2 = a_0^2 - [(\gamma - 1)/2]V^2 \tag{24}$$

For the flow considered the latter becomes

$$[(\gamma + 1)/2]a^2 = a_0^2 - [(\gamma - 1)/2]v^2 \tag{25}$$

and, hence, with the help of Eq. (15)

$$\frac{da}{dt} = -\left(\frac{\gamma - 1}{\gamma + 1}\right)\left(\frac{v\dot{v}}{a}\right) = -\left(\frac{\gamma - 1}{\gamma + 1}\right)\omega v \tag{26}$$

Therefore the acceleration formula becomes

$$A = 2v\omega + r\alpha = -2v\omega/(1 + \gamma) \tag{27}$$

and this may be further reduced to

$$A = (V_{cr}^2/r)(v/a_0)(r\omega/a_0) \tag{28}$$

in which V_{cr} is the so-called critical speed or the speed when $V = a$. In other words, the acceleration along a given radius vector is in magnitude inversely proportional to the distance from the pole and is in direction normal to the radius vector. Note that the curved flow is entirely supersonic (Eq. (18)) and that a fluid line segment, such as $\overline{cd}$ in Fig. 3, has a zero pressure gradient along r so that the constant pressure segment may be considered as moving locally in circular motion with a locally imposed uniform velocity a. The corner itself, however, is a region of infinite acceleration. This type of flow may be visualized as a borderline case between the minus and plus realms and might well be described as a flow of a zero realm.

General Flow

To compute the acceleration A at a point in a general flow pattern, a reference system can be selected so that the radial component of the acceleration is zero at the point considered, and, hence, with the aid of Eq. (6)

$$\dot{v} - r\omega^2 = 0 \tag{29}$$

$$-\frac{\partial v}{\partial r}r - v + \frac{r^2\omega}{a^2}(r\alpha + 2v\omega) - r\frac{\partial \omega}{\partial \theta} = 0 \tag{30}$$

If Eqs. 4, 16, 29 and

$$\dot{v} = (\partial v/\partial r)\,v + (\partial v/\partial\theta)\omega \tag{31}$$

are multiplied, respectively, by the multipliers v, r, $v/r\omega$, and $-v/r\omega$ and the results are added,

$$r\alpha + 2v\omega = r\omega\frac{\partial \omega}{\partial \theta} - \left(\frac{v^2}{r\omega}\right)\left(\frac{\partial v}{\partial r}\right) + \omega v \tag{32}$$

On eliminating $\partial w/\partial\theta$ between the Eqs. (30) and (32),

$$r\omega[(r\omega/a)^2 - 1](r\alpha + 2v\omega) = (\partial v/\partial r)[(r\omega)^2 + v^2] \tag{33}$$

and if $r\omega \neq a$,

$$A = \left[\frac{V^2}{(r\omega)}\right]\left\{\frac{\partial v/\partial r}{[(r\omega)^2/a^2] - 1}\right\} \tag{34}$$

in which V is the speed of the fluid at the given point.

A result immediately apparent is that, when $\partial v/\partial r$ is not small or zero, then large accelerations will be present when the acceleration component (the component of velocity colinear with the acceleration vector) of the velocity has a magnitude close to the local speed of sound. The radial flows showed this characteristic in the region of the circle in which $v = a$. The circular and corner flows are cases in which the derivative $\partial v/\partial r$ is zero. The accelerations are finite (except at the corner in the corner flow), even though in the corner flow the acceleration component of the velocity is in magnitude always equal to the local speed of sound. Supersonic flow in wind-tunnel channels is an experimental instance in which $\partial v/\partial r = 0$ when $\omega r = 0$.

It is evident (Fig. 4) that, if anywhere in the supersonic region of a compressible flow the acceleration component is greater in magnitude than the local speed

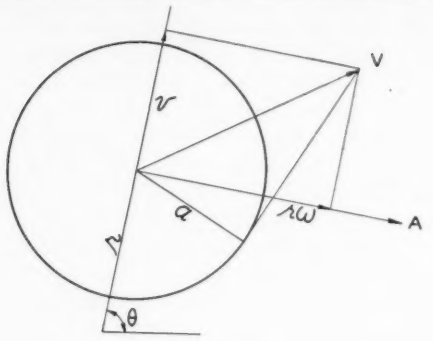

FIG. 4. Velocity-acceleration diagram.

of sound, the flow cannot pass continuously into a subsonic region unless the acceleration component of velocity takes on somewhere the local speed of sound. Near such a point, as has already been pointed out, it is necessary that $\partial v/\partial r$ be sufficiently small and approach zero as the point is approached if large accelerations are to be prevented. If in the supersonic region the acceleration component is less in magnitude than the local speed of sound, then the flow may pass into a subsonic region without incurring large accelerations, provided $\partial v/\partial r$ remains finite. It is merely a matter of not letting the angle between the velocity and acceleration vectors decrease too rapidly. Thus, on the forward portion of an airfoil which usually has a fairly large curvature, the angle between the velocity and acceleration vectors will be comparatively large and the flow may become supersonic in the presence of ordinary accelerations. If a sufficiently large angle between these vectors can be maintained on the airfoil, say by keeping the curvature large enough until the flow is again subsonic, then the accelerations will remain finite and shock wave should not occur. On the other hand, a sharp change in curvature somewhere on the airfoil aft and near the positions where the flow becomes supersonic will bring on an acceleration component of velocity equal to the local speed of sound, and then only suitable behavior of the gradient $\partial v/\partial r$ will prevent the formation of a shock wave.

REALMS OF FLOW

With the aid of Eq. (24) the acceleration formula (Eq. (34)), may readily be thrown into the form

$$A = \left[\frac{V^2}{(r\omega)}\right]\left(\frac{\partial v}{\partial r}\right)\left\{\frac{1 - (V/V_m)^2}{[(r\omega)^2/V_{cr}^2] + (v^2/V_m^2) - 1}\right\} \quad (35)$$

in which $V_{cr}^2 = 2a_0^2/(1+\gamma)$ is the square of the critical speed, while $V_m^2 = 2a_0^2/(\gamma - 1)$ is the square of the maximum attainable speed.

Examine Eq. (35) in the light of a hodograph plane that moves with the particle on its stream line and rotates so that one of its axes is always coincident with the acceleration vector. Fig. 5 is an acceleration-axis hodograph.

The velocity field is separated into two realms by the ellipse

$$[(r\omega)^2/V_{cr}^2] + (v^2/V_m^2) = 1 \quad (36)$$

The region inside the ellipse is one in which the elliptic form in the denominator of Eq. (35) is negative, while that outside the ellipse is one in which the form is positive. These regions have been correspondingly described as the minus and plus realms of flow. The physical significance of this separation may be gleaned by an examination of Eq. (35) for several variations of the parts of the formula.

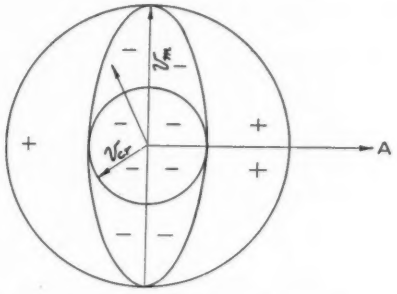

FIG. 5. Acceleration-axis hodograph plane.

Consider the following four alternatives exhibited in Fig. 6—a minus realm and

$$\frac{\partial v}{\partial r} > 0 \begin{cases} r\omega > 0 & A < 0 & \text{I} \\ r\omega < 0 & A > 0 & \text{II} \end{cases}$$

$$\frac{\partial v}{\partial r} < 0 \begin{cases} r\omega > 0 & A > 0 & \text{III} \\ r\omega < 0 & A < 0 & \text{IV} \end{cases}$$

The counterclockwise direction is regarded as positive in all cases.

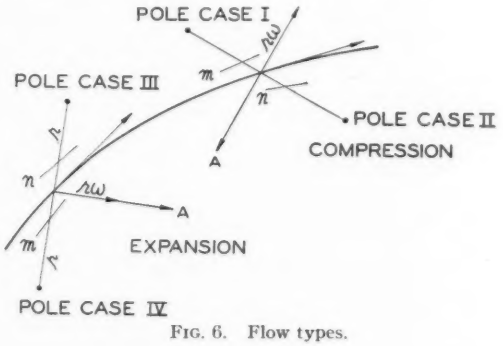

FIG. 6. Flow types.

In case I (Fig. 6) $(\partial v/\partial r) > 0$ and, hence, the particles on the constant pressure fluid line segment are separating and flowing against the pressure. Thus the flow is physically like that of case 1 of Fig. 1. Further, just as in case 1 (Fig. 1), large accelerations will be present when r is close to the local speed of sound. Similar findings may be established for the other three alter-

(Continued on page 231)

Medical Research in Some Aspects of Aircraft Design

WILLIAM E. RUSSELL,* JOHN R. ERWIN,† AND HUGH R. DEHAVEN‡

Boeing Aircraft Company and National Research Council

INTRODUCTION

IN PAST YEARS pilots could fly almost any plane that would rise off the ground with little more than the hazard of falling to obstruct their work. The rapid evolution of aircraft design has removed much of the hazard of falling but has introduced new hazards that have arisen with improvements. Changes in design have brought out forcibly that airplane performances are much superior to the physical abilities of the flight personnel who are using the new aircraft. It has also been brought out that certain changes in structural design will increase the possibility of survival from crashes.

Slowly the medical profession, in prewar periods, began research into the problems attending flight. With the advent of the war there came a stimulus for bettered plane performances, and the aircraft engineers have developed such superior planes that, beyond any doubt, the medical profession must exert itself to the utmost to increase the physiologic capacities of the flight personnel in order that the full potentialities of these airplanes may be utilized.

PHYSIOLOGIC LIMITATIONS

The aircraft engineers are well acquainted with all advances in plane design, and the pilots have experienced in part some of the new physiologic problems that have arisen. It may be of some interest to point out briefly the most important physiologic limitations that have developed. Better motors and construction have increased the speeds of horizontal flight past the 400-m.p.h. range and diving speeds in excess of 600 m.p.h. With these speeds there is a constant danger that the pilot may black out from cerebral anemia caused by sudden changes in the direction of motion. The rate of ascent of the airplanes has sharply increased and the ceiling of the planes has been raised into the realm of the substratosphere. Fast ascents have introduced the problem of aeroemphysema or bends, and the increased altitudes have introduced the problems of anoxia or oxygen lack and the constant danger of the extreme cold of high altitudes. Flying ranges and flight time have both been increased to such a point that flight personnel are spending long periods of time in flight. The increased working time, along with the problems of anoxia, noise, and vibrations, has introduced the question of chronic fatigue from flight. Heating systems and military installation of armament have increased the possibility of carbon-monoxide poisoning, and this is of some concern, especially since the airplanes now have enclosed cabins.

Many professional groups are constantly experimenting in the physiologic problems attending aviation. The Army and Navy have excellently trained physiologists and physicians who are working constantly to erase human limitations. The most eminent professional men in the country, under the auspices of the National Research Council, are lending their services to probe the mysteries of aviation medicine. The well-qualified medical staffs of the commercial air lines and the industrial physicians in the aircraft industries are each lending all the assistance possible in the pressing situation.

AVIATION MEDICINE IN THE AIRCRAFT INDUSTRY

The aircraft engineers will probably have more intimate contact with the industrial physicians on the questions of aviation medicine, and the industrial physician will act as the liaison between the engineers and the other professional groups that are experimenting in the fields. Industrial medicine in the aircraft industry has a vital part in the maintenance of the health of the flight personnel. The flight personnel are the group upon which the engineers are depending for accurate interpretation of their work, and the engineers should be thoroughly acquainted with some of the problems attending their care.

There are several factors that make the practical application of aviation medicine to the flight work of an aircraft industry somewhat unique:

(1) The group encountered consists of a variety of differently trained personnel, such as pilots, flight engineers, flight inspectors, etc.

(2) The flight personnel in industry comprises men of all ages, temperaments, and physical abilities.

(3) Test flying is in a class by itself in that the work consists of taking unstandardized equipment and checking its performance for possible use in military or commercial purposes. Pilot errors may have a far-reaching effect on the interpretation and may be a cause for acceptance or rejection.

Presented at the Physiologic Problems Session, Eleventh Annual Meeting, I.A.S., New York, January 25–29, 1943.

* Medical Supervisor, Boeing Aircraft Company.

† Assistant Medical Supervisor, Boeing Aircraft Company.

‡ Crash Injury Research Project, National Research Council.

(4) Flight personnel in this day are not only the guinea pigs for testing design but are also the men who use experimental physiologic equipment in order to push themselves beyond former accepted physiologic limits to prove the full capabilities of the plane. Failure on the part of the personnel because of physiologic problems may have a marked effect upon future designs.

Health of Flight Personnel

In the maintenance of the flight personnel so that they can adequately conduct their work, there are two things of basic importance. An adequate physical examination must be regularly conducted and an adequate educational program forms an equally important part. These physical examinations must be suited not only to the type of occupational groups doing the flying but also must be suited to the specific type of flying—for example: (1) those doing occasional flying, such as mechanics and production engineers; (2) those flying considerably but not involved in actual pilot operations; and (3) those doing considerable flying and on whom depends the safety of the plane, such as pilots, copilots and crew leaders.

The types of flying can roughly be grouped into: (1) low altitude or flights under 15,000 ft. and (2) high-altitude flights or those from 15,000 up to 50,000 ft. or more.

The basic examination must be complete with such special investigation as seems indicated for the group or type of flying. Initially, this insures that the personnel are capable of safe flight, and repeated examinations rule out the possibilities of pathologic conditions developing which might be detrimental to the continuance of flying. Each aircraft industry has had to permanently rule out individuals from flying because of cardiac, respiratory, or other serious medical conditions. Individuals have temporarily been grounded because of acute infectious diseases such as colds and sore throats, and occasionally it is necessary to ground one because of anemia.

The educational program must include a study of: (1) the physiology of respiration and circulation as a basis of understanding anoxia and aeroemphysema; (2) the principles of oxygen masks, oxygen systems, and flowmeters; (3) the relationship of exercise and diet to the work; and (4) the practical indoctrination in pressure chambers to show effects of physiologic problems and to instruct the men in safety procedures under simulated flight conditions.

Expansion of High-Altitude Flying

The Boeing Aircraft Company has played a vital part in the expansion of high-altitude flying under the supervision of the late Edmund T. Allen, Director of Flight and Aerodynamics, and A. C. Reed, Chief of the Flight Test Unit. This organization is unique in that it is the only group in the country thus far to have taken large crews repeatedly to high altitudes and to have flown there for extensive periods. Experience has resulted in the establishment of a number of regulations designed to safeguard the lives and health of the flying personnel who are engaged in high-altitude flight. These rules are in some part a reiteration of what has been mentioned previously as a maintenance program for the flight personnel, but they illustrate how the rules have been adapted to high-altitude work. Briefly these are as follows:

(1) Oxygen is kept available in airplanes on all flights. It is used on all flights above 10,000 ft. and at the present only the B.L.B. No. 12 mask is used on flights between 25,000 and 40,000 ft. No flight shall be made above 40,000 ft. without the use of a pressurized cabin, a pressurized suit, or a pressurized oxygen mask.

(2) Crew preparations: (a) physical examinations; (b) lectures, demonstrations, and study of physiologic and equipment problems; (c) practice and drills outside and inside the chamber; and (d) review of procedures in preflight conference.

(3) Ground check-off list of safety measures is to be filled out completely by each crew member before each high-altitude flight.

(4) Denitrogenation will be required on all flights above 25,000 ft. This will consist of at least 45 min. of oxygen, of which at least 30 min. time will be spent in exercise the equivalent of walking at the rate of approximately 3 m.p.h. (a) The personnel wear as routine equipment helmets with built-in earphones, goggles, gloves, jumper suit, bailout bottle, bailout mouthpiece, emergency kit, oxygen mask B.L.B. No. 12, parachute, life jacket, and mukluks.

Flight Test Crews

Using the above procedures, the Boeing flight test crews have established the following in all experimental planes, from July 21, 1940, to November 30, 1942:

(1) The total airplane flight time at all altitudes shall be 956.14 hours.

(2) The total flights shall be 453 hours.

(3) The total number of men routinely engaged in high altitude test flights shall be 69. (Note: To be considered as routinely engaged, it is necessary arbitrarily for a man to have spent at least 3 hours at 35,000 ft.)

(4) The number of flights in which an altitude of 29,000 to 34,000 ft. was reached shall be 72.

(5) The number of flights in which an altitude of 34,000 ft. or above was reached shall be 67.

(6) The collective personnel's flight time, spent at altitudes of 29,000 to 34,000 ft. shall be 342.20 hours.

(7) The collective personnel's flight time, spent at altitudes of 34,000 ft. or above, shall be 977.07 hours.

Research on High-Altitude Planes

Various limitations have been encountered during the experimental work on high-altitude planes and various research is under way not only at the Boeing Company but also in the various professional groups to reduce these limitations. Because of military necessity, specific information cannot be revealed by the Company, but the following statements can be made:

Cold

There has not been the problem of cold in the B-17 because the heating system has proved to be adequate.

Aeroemphysema

Various research, plus the practical experience of Boeing, substantiates the contention that with use of oxygen and exercise almost complete immunity can be had from aeroemphysema or bends. This has been proved definitely enough so that when there is a case of bends it is believed that the crew have been lax in their preparation.

Noise

The noise level has been checked under various conditions in the soundproofed and unsoundproofed portions of the Flying Fortress with results that indicate there should not be any chronic hearing loss. Medical examination of the flight personnel has not revealed any chronic hearing damage. It is felt that the noise and vibration cause a certain measure of fatigue, but how much has not yet been concluded.

Oxygen

Tests have been performed revealing no appreciable concentration of carbon monoxide during flight conditions. Studies are being conducted in reference to chronic flight fatigue, but so far no practical routine for operation of the pilots has been set up. There have been various studies on oxygen equipment, including a limited amount of study on certain demand types of oxygen masks. There is an excellent possibility that certain forms of demand masks will greatly increase the safe operational altitude above that of our existing equipment.

Pressurizing Equipment

It is the feeling of the Flight and Aerodynamics group at the Boeing Company that pressurized suits, pressurized cabins, or some type of pressure oxygen mask offer the answer for high-operational flights. There are certain limits to each type of equipment, but favorable studies are under way, of which only mention can be made. It has been found that pressurized suits are large and bulky and that the suit is apt to lose its pressure when the pilot is moving around in it. There is a definite limit on how much pressure can be built up in a suit and this will limit its use. Pressurized cabins offer a hope for high altitudes, in fact high enough so that should the pressure fail there is a probability of present oxygen equipment not sustaining life, with the death being from anoxia. Since pressurized cabins will be used under military conditions, there has been considerable interest aroused as to the possibility of a quick loss of pressure or, as it has been termed, explosive decompression. If pressure masks will permit temporary to long operations up to the altitudes the pressurized cabin will sustain, then the problem of safety will be solved, but until a new mask has been standardized there is a definite physiologic limitation to the pressurized cabin.

There have been newspaper reports of German flights up to 50,000 ft. or more and also reports of British flights up to the same altitudes to shoot these German craft down. It is difficult to theorize on newspaper reports, but the Boeing Flight and Aerodynamics group feels that undoubtedly the Germans have developed pressurized cabins and that the reported flights must have been made in them. The fact is pertinent that, in order not only to match our enemies but also to better their efforts, there must be the fullest advancement of aircraft design and advancement of medical experimentation so that aviators can utilize the superior designs created.

Crash Injuries

It is becoming more apparent as the war progresses that skilled aviators must be preserved at all costs. Over the past years little has been done for the flier who finds himself facing a crash. Designers have been concerned with improving the efficiency and flight characteristics of aircraft and, when crashes occurred, death and injury have been the accepted result.

Combat flight and war transport have led to much thought on the hazards of crash landings in water, jungle, and desert. Injury under these conditions presents formidable problems. To minimize this danger an extensive survey has been undertaken by the Army, Navy, R.A.F., and Civil Aeronautics Board, who are extending their cooperative findings to a research group in the National Research Council. Through this joint effort, survivable aircraft injuries are being closely studied and related to the structure that causes them. As a result, many problems of repeated unnecessary injury are coming to light.

Anyone who has viewed the results of an extreme aircraft accident could hold no illusions about modifying the injuries sustained in this type of crash. The aircraft disintegrates and the injuries are in accord with the general destruction. Unfortunately, as wing loadings increase, this type of accident holds in the largest proportion. But the constantly increasing use of aircraft confronts designers with an ever enlarging group of crashes that are not extreme and in

which a substantial portion of the cockpit or cabin remains intact. This is the type of crash that can be termed marginal. It is on the edge where injury and fatality may or may not occur. It differs from the extreme crash in its physiologic result, for, whereas the extreme crash tends to tearing, crushing, and grinding injuries because of collapse of the plane's structure, the marginal crash yields simpler results that are inflicted by being thrown against objects in the portions of the plane which remain intact. Survival here is a matter of chance, depending upon how the body is thrown.

Force and Restraint

The force to which the victims of a marginal crash are exposed is largely unexplored. The fact that the body of the plane holds together indicates that it is not extreme—otherwise intact structure would not be present. A tail gunner who survived an extreme crash into the side of a mountain in which seven were killed relates that when he heard timber crashing he remained seated in the gunner's seat and leaned well over, protecting his face with his arms and helmet. When the final impact came the force merely threw him into an upright position, bruising his back and shoulders slightly and giving him a "crick" in the neck. It is nothing less than amazing that a crash fatal to seven should have caused merely a crick in the neck for the eighth person. Others might have survived if they had not been thrown against the structure during the force interval. The tail gunner came through safely because his body was restrained, even though his head and neck were not too well supported.

The importance of proper restraint is evidenced in another incident in which an airliner was involved in a minor landing accident. The pilots and passengers came out of this accident without material injuries, but the hostess standing in the rear was unrestrained. She kept going and overtook the structure after it had come to a stop. The effect was that she was thrown the length of the cabin, gaining speed in a relative acceleration to the plane over this distance. Her head struck a stress member and she stopped against the door to the pilots' compartment. She was unconscious for more than 20 days.

These two instances—one of survival in an extreme crash and the other of severe injury in a minor one—are outstanding examples of how force works for injury or survival in an aircraft accident. Unless the physical facts of force are held in mind, the results just mentioned seem confusing but are, in fact, simple. The tail gunner in the first instance hit nothing. He was pressed against structure during the crash and survived a high rate of deceleration because of good distribution of pressure. He avoided impact, was pressed against the structure, and moved with the structure until the force was expended. Stunt drivers crash cars daily and survive through use of this fact. It seems to work without any practical limit where structure provides the possibility. From the point of view of physics, the answer appears to be that the pressure between the body and a supporting surface is largely compensated and, as a result, virtually ceases to exist as an injury factor. Where this occurs, cases are on record of falls from heights of 100 to 150 ft. onto structure apparently inadequate for human safety not only with survival but often with minor injuries. To cite one instance of pressure compensation, a woman jumped from the tenth floor window of a hotel and landed flat on her back in a garden plot 93 ft. below. The facts were carefully investigated and reported along with eleven other instances of falls from height in a recent paper.[1] Her speed when she struck the ground was estimated at 50 m.p.h., but she sustained no internal injuries; nor was there any apparent head injury or loss of consciousness. A bruise on her forehead, a fractured wrist, and one fractured rib were the only force results in evidence, and it is believed probable that her wrist was actually fractured by striking across her forehead. Her force during the deceleration of this 50-mile speed was close to 200 times the force of gravity when the earth packed hard and stopped her. Yet the victim of this exposure to extreme force was out of the hospital in twelve days. As the tail gunner referred to could not have been exposed to more than a fraction of this force, his survival with proper distribution of pressure is understandable. On the other hand, the hostess who was thrown freely suffered severe head injuries.

Head Injuries

Of all aircraft injuries, head injuries are the most common cause of fatality. The reason they occur so frequently is based on simple physical facts. The head weight is about 10 lbs. With the velocity obtained from a 1-ft. fall, the head will store 10 ft.lbs. of energy, which can give a pressure close to 2,000 lbs. to the square inch if localized by a knob, tubing, or projection in an area of 1 sq.cm. It is not remarkable, therefore, that repeated instances of fatality in aircraft accidents occur from localized injury to the head without another mark on the body.

Structures to Prevent Injuries

There are today many types of structures used in aircraft which have low injury potential, but there are also structures in use which are packed with injury hazard. Where the true dividing line between good and bad structure lies is still unknown. There are types of rudder pedals, for instance, which properly support the feet and cancel out many foot and leg injuries inherent to others, and there are windshield supports that have been repeatedly demolished by the force of the head instead of causing fatal head injury. Certain types and placement of seat belts

and restraining harnesses must be giving far better results than others.

Experimentation

In order to get at the facts, plans are under way to crash planes under controlled conditions, using high-speed cameras and proper instrumentation to record the results. Dummies will be used to represent the throw of the body and reduce causes of injury to slow motion. Unfortunately, dummies can yield no true physiologic data and, as human experimentation is out of the question, field surveys have been undertaken by the Army, Navy, and Civil Aeronautics Board in order to study the physiologic evidence from actual crash conditions. These surveys include data on the aircraft; estimates of the speed and angle of the crash; condition of the cockpit or cabin; and data on the seats, belt fastenings, and shoulder harnesses. Notes will be made of the force and direction in which victims were thrown and of the nature and placement of objects inflicting injury in survivable accidents. The benefits and effects of improved safety belts and restraining harnesses will come under close observation.

When the reports from these efforts and from similar work now going forward in England are assembled, engineers will have for the first time an extensive source of information on which to base their estimates of the best available structure to meet the problems of crash injury in order to enhance safety under crash conditions in the future.

REFERENCE

[1] Hugh R. DeHaven, *Mechanical Analysis of Survival in Falls from Heights of Fifty to One Hundred and Fifty Feet*, War Medicine, Vol. 2, p. 586, July, 1942.

(*Continued from page 226*)

natives. Thus it is evident in these cases that even though the flow may be supersonic, the fluid particle responds to its physical surroundings as in an ordinary subsonic flow.

It is readily shown that in the plus realm the fluid responds to its physical surroundings as in the cases 3 and 4 of Fig. 1. The figures would be like those in Fig. 6, with the channel lines m, n rotated so that their closing tendency is reversed to correspond to changes in sign of $\partial v/\partial r$. Acceleration-axis hodograph curves of stream lines in the radial flows will lie entirely in the A axis; the subsonic flows, in the minus realm; and the supersonic flows, in the plus realm. Stream lines in the circular flow have a point representation on the vertical axis of the hodograph plane and, hence, the flow is entirely of the minus realm. Stream lines of the corner flow will have hodograph curves that lie entirely on the hodograph ellipse, and, hence, the flow may be designated as of the zero realm.

Acceleration-axis hodograph curves are readily plotted from corresponding curves in the ordinary hodograph plane by measuring, in the latter, the angles between the velocity radius vectors and the tangents to the curves. These angles are the angles between the velocity and acceleration vectors.

Finally, it will be noted that when the hodograph of a stream line comes near or crosses the hodograph ellipse then large accelerations may be expected unless the velocity gradient defined by the directional derivative $\partial v/\partial r$ takes on suitable values.

REFERENCES

[1] von Kármán, Th., *Compressibility Effects in Aerodynamics*, Journal of the Aeronautical Sciences, Vol. 8, No. 9, pp. 337–355, July, 1941.

[2] Taylor, G. I., and Maccoll, J. W., "The Mechanics of Compressible Fluids," Div. H; Durand, W. F., *Aerodynamics Theory*, Vol. III; Julius Springer, Berlin, 1935.

23 2

SUGGESTIONS FOR CONTRIBUTORS TO THE PUBLICATIONS *of the* INSTITUTE *of the* AERONAUTICAL SCIENCES

The Institute of the Aeronautical Sciences invites both members and nonmembers from any country to submit papers for publication in the JOURNAL OF THE AERONAUTICAL SCIENCES and the AERONAUTICAL ENGINEERING REVIEW. The Institute, following the practice of other societies, does not pay for contributions.

The following directions for the preparation of papers, if followed by authors, will save correspondence, avoid the return of papers for changes, minimize the work of preparation for the printer, and save the expense due to the charges made for "author's corrections."

MANUSCRIPTS: Papers must be written in English, in original typewriting on one side only of white paper sheets, consecutively numbered, and be double or triple spaced with wide margins. Manuscripts should be prepared with great care so that they will be typographically accurate. Paragraphing should be given special attention. Papers should be written in the third person, reference to the writer being made as "the author." Avoid the use of the words "I," "we," and "you." Blueprint copies of papers are unacceptable as it is impossible to mark directions to the printer on them. Correcting, changing, or adding to papers after they are in type is costly. It is, therefore, imperative that papers submitted be in final form. Typographical errors may be corrected on proofs, but if authors wish to add material, they may do so at their own expense. In mailing, drawings may be rolled, but manuscripts should be sent flat. Send by first class mail (register if you wish for your own protection) to the Editorial Office, Institute of the Aeronautical Sciences, 1505 RCA Bldg. West, 30 Rockefeller Plaza, New York 20, N. Y. All manuscripts will be examined by the Editorial Committee and by the Editor. Authors will be advised as promptly as possible whether the paper is acceptable for publication.

TITLES: The title of the paper should be brief. The name and initials of the author should be written as he prefers. The use of the full name of an author is advocated because of the frequent duplication of initials and surnames which sometimes makes it difficult to establish the identity of the author. This is particularly important for large annual indexing and abstracting services. All titles and degrees or honors are omitted. The name of the organization with which the author is associated should be placed after his name on a separate line. The date on which the paper is received will be inserted by the Editor.

SUMMARIES OR ABSTRACTS: An abstract to be printed at the beginning should accompany each article. It should be adequate as an *index* and as a *summary*. It should contain a statement of major conclusions reached, since summaries in many cases constitute the only source of information used in compiling scientific reference indexes. Abstracts printed in other journals, especially foreign, in most cases, consist of summaries from printed papers. The summary should explain as adequately as possible the major conclusions to a nonspecialist in the subject. The summary should contain from 100 to 300 words, depending on the length of the paper.

SUBHEADINGS: Subheadings should be inserted by the author at frequent intervals. The work of editorial preparation will be simplified by the author providing many subheadings. Owing to the breaking of columns and the insertion of illustrations, some of the subheadings may have to be omitted.

SHORTENING OF PAPERS: Some papers, at the end, fill in only a portion of a page. This leaves much wasted blank space as succeeding articles are started at the top of a page. Authors should indicate by notation on the left-hand side of the page what matter may be omitted when "runovers" occur. This request is important as the Journal cannot afford in the future, as it has in its earlier issues, to have blank half pages or more at the end of papers.

MATTER USUALLY DELETED: Acknowledgments of assistance in preparation of paper, except by collaborators. Photographs or illustrations of little technical interest and not showing advances in general practice. Too detailed tabular matter (general results of such tables may be included in the text). Lengthy descriptions of materials or processes or of preliminary experiments or theories that preceded final results; salient features only are of interest.

REFERENCES AND FOOTNOTES: References should appear as footnotes only, numbered consecutively, grouped together at the end of the manuscript. The arrangement should be as follows: (for books)—[1] Durand, W. F., *Aerodynamic Theory*, 1st Edition, Vol. 1, p. 23; Julius Springer, Berlin, 1934. (For magazines)—

[1]Englund, C. R., Crawford, A. B., and Mumford, W. W., *Some Results of a Study of Ultra-Short-Wave Transmission Phenomenon*, Proc. I. R. E., Vol. 20, No. 12, pp. 481 and 482, March, 1933. Please give author, title, edition, volume, page, publisher and date of publication as indicated. Omission of one required fact causes much extra editorial work and possible inaccuracies. All references are grouped at the end of the article.

ILLUSTRATIONS: Illustrations should accompany manuscripts and each should always be referred to in the text, preferably by number. Drawings or graphs should not be larger than 12 × 16 inches, and must be made with jet black India Ink on white paper or tracing cloth, the latter being preferred. *Do not use typewriter for lettering.* The smallest lettering on 8 × 10 inch figures should be no less than 1/4 inch high. Cross-section paper (white with black lines) may be used, but should not have more than 4 lines per inch. If finer ruled paper is used, the major division lines should be drawn in with black ink, omitting the finer divisions. In the case of finely ruled paper, only blue-lined paper can be accepted. *Tracing paper and blueprints* are not acceptable. Lettering and all markings must be large enough to be readable after reduction. Mail rolled or flat, never fold. Drawings that cannot be reproduced (including pencil drawings) will be returned to the author for redrawing, thus delaying publication of the paper. Photographs should be very distinct and show clear black and white contrasts. They must be on glossy white paper. Avoid round and oval photographs.

CAPTIONS AND LEGENDS: Legends or captions must accompany each drawing or photograph submitted. If written on the drawing or photograph, they should be placed below and well outside the part to be reproduced. It is better to place them on separate sheets of paper pasted to the back of the drawings or photographs. Each table should have a caption such as Table 1, Table 2, Table 3, etc. Captions should be complete in themselves so as to make the data intelligible to the reader without reference to the text. A duplicate list of captions for figures should be included as the last page of the manuscript. Use "Fig. 1" (not Figure 1), Figs. 3 and 4, etc., in both the text and the numbering of illustrations. In the text, "Eq. (1)," or "Eqs. (1) and (2)" are preferable to "Equation (1)." In captions and legends, except for "Fig." and "Eq." and table headings, write all words in full; do not abbreviate. Avoid placing explanatory written matter in the drawings; it should be in the text.

MATHEMATICAL WORK: Only the simplest formulas should be typewritten; all others should be carefully written in pen and ink, the writing to be large enough so that ample room is provided to mark mathematical matter for the printer. A considerable space for marking should be allowed above and below all equations. All complicated equations should be repeated on separate sheets with plenty of space left for marking. The solidus should be used for simple fractions appearing within the text. Make all expressions clear to the typesetter. Greek letters used in formulas should be clearly designated by name on the margin of the manuscript. All symbols should be clearly written and carefully checked. The difference between capital and lower-case letters should be clearly distinguished and care taken to avoid confusion between zero (0) and the letter (o), between the numeral (one) and the letter (ell) and the prime (′), between alpha and a, kappa and k, u and mu, v and nu, n and eta. All subscripts and exponents should be clearly marked and dots and bars over letters or mathematical expressions should be avoided. Avoid complicated exponents and subscripts. When it is necessary to repeat a complicated expression, it should be represented by some convenient symbol.
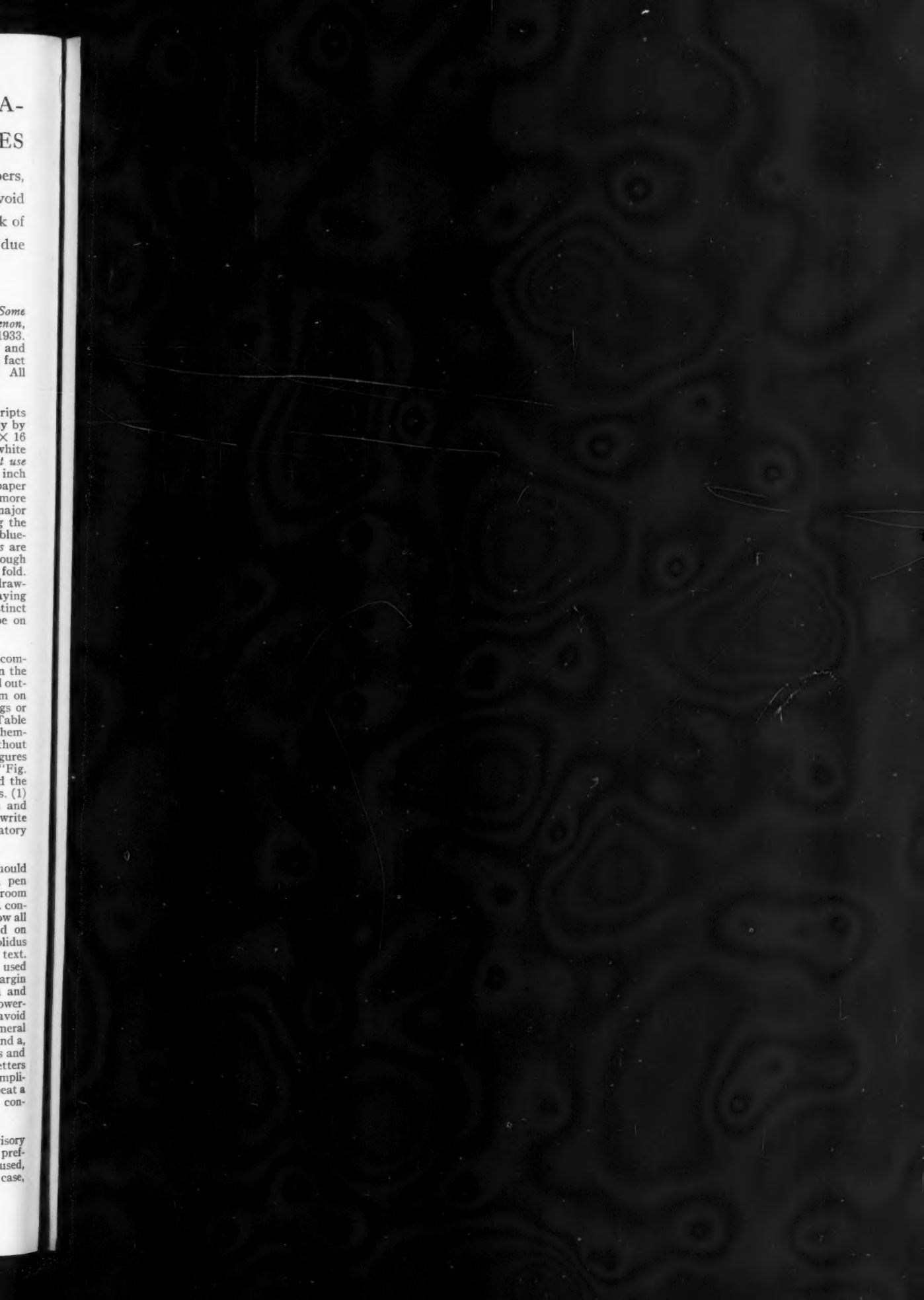
NOMENCLATURE AND ABBREVIATIONS: The National Advisory Committee for Aeronautics Nomenclature should be used in preference to any others. Standard abbreviations should be used, and it should be noted that most abbreviations are lower case, such as m.p.h., b.m.e.p., i.hp., b.hp., hp., . . . etc.